QATAR UNIVERSITY

COLLEGE OF ARTS AND SCIENCES

"SOURCES AND DISTRIBUTION OF SUSPENDED PARTICULATE MATTER (SPM) USING STABLE ISOTOPES IN THE CENTRAL ARABIAN GULF"

BY

JASSEM ABDULAZIZ K. H. AL-THANI

A Thesis Submitted to

the College of Arts and Sciences

in Partial Fulfillment of the Requirements for the Degree of

Masters in Environmental Science

June 2020

COMMITTEE PAGE

The members of the Committee approve the Master's Thesis of
Jassem Abdulaziz Al-Thani defended on 10/05/2020.

Dr. Yousria S. Soliman
Thesis/Dissertation Supervisor

Dr. Ebrahim A. S. Alansari
Thesis/Dissertation Co-Supervisor

Dr. Ibrahim A. Al Maslamani
Committee Member

Dr. Oguz Yigiterhan
Committee Member

Approved:

Ibrahim AlKaabi, Dean, College of Arts and Sciences

ABSTRACT

AL-THANI, JASSEM, A., Masters, May, 2020, Environmental Sciences

Title: Sources and Distribution of Suspended Particulate Matter Using Stable Isotopes in Central Arabian Gulf.

Supervisor of Thesis: Yousria, S. Soliman; Ebrahim, M. Al-Ansari

Suspended Particulate matter (SPM) (>0.45μm) plays a significant role in the global carbon cycle. Hence, we measured changes in concentrations of SPM with depth and at distances from shore in the exclusive economic zone of Qatar (EEZ). Signatures of stable isotopic analysis and elemental composition of organic carbon and nitrogen were used to assess sources of SPM during summer of 2019. Samples of SPM were collected from three transects crossing the EEZ representing different depths. Hydrodynamic parameters including salinity, density, water temperature, and DO were measured to assess effects of different water masses on the distribution of the SPM. The study investigated the relation between Chl-a concentration and SPM in order to identify the non-algal SPM sources. The isotopic composition of SPM showed a distinct carbon isotope depletion and a relative nitrogen enrichment, except for a few locations were nitrogen was depleted ($\delta^{15}N \sim 0$). The dissolved nutrients and chlorophyll-a showed distinct trends with depth and with distance from shoreline. Trends of Chl-a indicated that the shallow central Arabian Gulf is relatively productive with high chlorophyll-a and nutrients at the shallower sites within 40 km from the coastline. The SPM's stable isotope composition confirmed that phytoplankton is a prominent source for SPM in the Gulf with an average $\delta^{13}C$ of about 18.56 ‰. On the other hand, $\delta^{15}N$ signatures in SPM showed that nitrogen from nitrogen-fixation play a significant role in supporting new nitrogen sources and primary productivity in the central Arabian Gulf at the north eastern region of the EEZ of Qatar.

DEDICATION

To my family and my master's thesis supervisors, who motivated me throughout the hard work on this study.

ACKNOWLEDGMENTS

I am very thankful and grateful to both supervisors of my M.Sc. thesis, Dr. Yousria S. Soliman and Dr. Ebrahim A.S. Al-Ansari, for their invaluable advice, motivation, patience and help throughout this project and in my thesis work. I highly appreciate their constant encouragement with this thesis, motivating an unyielding drive to do the best work possible for such an important project. Their help in this project made everything possible from their aid in arranging field trips to making sure that I am always driven to do my best and to pour a lot of hard work onto this thesis. This project began as a very interesting idea for a project, and they helped make it a reality despite hardships throughout the period of doing this project, providing essential help and guidance. I also thank my committee members Dr. Ibrahim Al-Maslamani and Dr. Oguz Yigiterhan for their guidance and advice. Great thanks are extended to the crew of the R/V Janan and the ESC team that came during the field trips and greatly helped including Caesar Sorino, Hamood Alsaadi, Mark Chatting and Muhammed Pindath. I would like to thank DM Estremadura and Abdul-Ali Moghadasi for their help in the lab from sampling to help in analysis. I would also like to extend my gratitude to the Department of Biological and Environmental Sciences for providing the facilities for the work on this project and the Environmental Sciences Center for providing the R/V Vessel Janan. The work of Dr. E. Brendan Roark and Mr. Chris Maupin and the Stable Isotope Geosciences Facility at Texas A&M University, College Station is appreciated in analyzing stable isotopes of the samples and providing the methodology. Finally, I would like to thank and express my greatest gratitude to my family, especially my mother, who were patient, encouraging and motivating, always pushing for giving my best in everything I do in my life, career and studies.

TABLE OF CONTENTS

DEDICATION……iv

ACKNOWLEDGEMENTS……v

LIST OF TABLES……viii

LIST OF FIGURES……ix-xi

LIST OF ABBREVIATIONS ……...xi

CHAPTER 1: INTRODUCTION AND LITERATURE REVIEW……..…….....1-7

1.1. Introduction……...…….....1-3

1.2.Background/Literature Review…….3-6

1.3.Research Objectives…….....6

1.4.Significance and Reasoning of the study……..6-7

CHAPTER 2: STUDY AREA AND BACKGROUND INFROMATION…...……..8

CHAPTER 3 MATERIALS AND METHODS ……..…..9-24

3.1. Field Sampling and Sampling Processing…..……...……12-15

3.1.1. Hydrography and Physiochemical Parameters Field Measurements……...……..12

3.1.2. Seawater dissolved Oxygen……..…..……13

3.1.3. Nutrients (Nitrate, Nitrite, Phosphate, Silicate and Ammonia)…… …..13

3.1.4. Suspended Particulate Matter (SPM) and Chlorophyll-a……..13-15

3.2. Samples Processing and Analysis…….……....16-24

3.2.1. Dissolved Oxygen (DO)……...……..16

3.2.2. Dissolved Nutrients NH_4^+, NO_3^-, NO_2^-, PO_4^{3-} and SiO_4^{2-})……....16-20

3.2.2.1. Ammonia (NH_4^+)……...18

3.2.2.2. Nitrite (NO_2^-)……..…19

3.2.2.3. Nitrate (NO_3^-)……...19-20

3.2.2.4. Reactive Inorganic Phosphate (PO_4^{3-})……...20

3.2.2.5. Dissolved Inorganic Reactive Silicate (SiO_4^{2-})…….20

3.2.3. Chlorophyll-a……..……..20-21

3.2.4. SPM Nitrogen and Carbon Stable Isotopes……...22-23

3.2.5. Analysis of Data and Graphical Techniques…. ……....24

CHAPTER 4: RESULTS …….25-44

4.1. Hydrography and Physiochemical Parameters…….25-27

4.2. Dissolved Oxygen…….28-29

4.3. Nutrients (Nitrate, Nitrite, Phosphate, Silicate and Ammonia)……30-35

4.3.1. Ammonia……...30-31

4.3.2. Nitrate……31-32

4.3.3. Nitrite……32-33

4.3.4. Phosphate……..…33-34

4.3.5. Silicate……...34-35

4.4. Chlorophyll-a……35-37

4.5. Suspended Particulate Matter and Stable Isotopes of Carbon and Nitrogen……37-38

4.5.1. Suspended Particulate Matter (SPM)……37-38

4.5.2. Particulate Organic Carbon and Nitrogen (POC and PON)……..39-40

4.5.3. Carbon to Nitrogen Ratio (C:N)……41-41

4.5.4. Carbon and Nitrogen Stable Isotopes ($\delta^{13}C$ and $\delta^{15}N$)…….42-44

CHAPTER 5: DISCUSSION……45-51

CHAPTER 6: CONCLUSION……...52

REFERENCES……..53-59

LIST OF TABLES

Table 1. Information of eighteen offshore sampling locations within the waters of Qatar's EEZ, including station name/ID, total depth and distance from shore……11

Table 2. Detection limits for measured nutrients ……..…….....18

Table 3. Summary of range and mean values of temperature and salinity measured in the Exclusive Economic Zone (EEZ) of Qatar. The data is for the summer season (September 2019)…… …….....29

Table 4. Summary of range and mean values of pH and density in the Exclusive Economic Zone (EEZ) of Qatar in the late summer (September 2019)……. …….30

LIST OF FIGURES

Figure 1. The Oceanic Nitrogen Cycle (left) (Sollai et al, 2015), and the Oceanic Carbon Cycle, which shows the complex pathways and forms of carbon that exist in the marine environment, from inorganic to organic, and living to non-living forms of carbon (Oceans and the Carbon Cycle, https://serc.carleton.edu/eslabs/carbon/6a.html).....3
Figure 2. Map of the hydrography of the Arabian Gulf (Limits in the Seas, 1981) …..…….....8
Figure 3. Map of sampling stations in the Exclusive Economic Zone (EEZ), Qatar, in the central Arabian Gulf.……...……..10
Figure 4. *RV* Janan (left) and the rosette fitted with a dozen Teflon-coated Niskin bottles being lowered onto the water column of the sampling location (right). 12
Figure 5. Preparation of the Whatman GF/F filters by weighing (left), ashing (middle), then labeling and storage of the filters (rigth) ……..….....14
Figure 6. Sampling and pre-filtration and filtration of SPM: the filtrate retained on the NITEX screen (120-µm mesh size) when pre-filtered samples (top left), the pre-cleaned filtration apparatus for the collection of chlorophyll and SPM (bottom left), the filtration of the seawater samples (top left), and SPM retained on the pre-combusted GF/F filter (bottom right)..……..….15
Figure 7. SPM on GF/F membrane filter. Sample were dried at 60 °C, placed in labeled, aluminum foil tubes in a pre-combusted glass jars.……..….....24
Figure 8. Temperature-Salinity plots by sample (a) and by depth (b), showing different water masses in the EEZ of Qatar.……..…….....26
Figure 9. Density (σt) in three main sampling depth zones (surface, mid-depth and near bottom water).…….....…….....27
Figure 10. Seawater pH down transect “A” extending from south to north of EEZ, showing an increase from the south (A1) to north (A9)..…….....27
Figure 11. Surface salinity (psu) of seawater down transect “A” extending from south to north of EEZ, showing a clear decrease in salinity from the south (A1) to north (A9)..…….....27
Figure 12. Change in dissolved oxygen (DO) in in the study area (mL/L) with depth (surface, mid-depth and near-bottom water) ……....28
Figure 13. Change of dissolved oxygen (DO) (mL/L) with depth (m) (left) and with distance from shore (right)…….. ……....29
Figure 14. Dissolved Ammonia (NH_4^+) in seawater (µM) with depth as surface, mid-depth and near-bottom water.…….....31
Figure 15. Dissolved Ammonia (NH_4^+) in seawater (µmol/L) with depth (m), with no discernable trend (a), and along distance from shore (km) (b)… ……...……31
Figure 16. Dissolved Nitrate (NO_3^-) in Seawater (µM) with depth zone in surface, mid-depth and

near-bottom water.…….…… …….....32
Figure 17. Dissolved Nitrate (NO_3^-) in Seawater (µmol/L) plotted with depth (m) (a), and with distance from shore (km) (b)…...…….…….…….....32
Figure 18. Change in dissolved Nitrite (NO_2^-) in Seawater (µM) with three main depths, (surface, mid-depth and near-bottom sampling depth) ……..…….....33
Figure 19. Dissolved Nitrite (NO_2^-) in Seawater (µmol/L) plotted with depth (m) (a), and with distance from shore (km), showing a quadratic trend (b)……..…….....33
Figure 20. Dissolved Phosphate (PO_4^{3-}) in Seawater (µM) with three main depth zones (surface, mid-depth and near-bottom water)…….....34
Figure 21. Dissolved Phosphate (PO_4^{-3}) in Seawater (umol/L) plotted with depth (m) (a), and with distance from shore (km) (b). ……..…….34
Figure 22. Dissolved Silicate (SiO_4^{2-}) in Seawater (µM) in three main depth zones (surface, mid-depth and near-bottom water)……..…….....35
Figure 23. Dissolved Silicate (SiO_4^{-2}) in Seawater (µmol/L) changes with depth (m) (a), and with distance from shore (km) (b) …….…….…….....35
Figure 24. Chlorophyll-a (mg/m^3) concentration with distance from shore (km) (a), and with depth (m) (b)……..…….....36
Figure 25. Changes in chlorophyll-a (mg/m^3) concentrations with nitrate (NO_3^-) (µmol/L) (a), phosphate (PO_4^{-3}) (µmol/L) (b), silicate (SiO_4^{-2}) (µmol/L) (c), and temperature (°C) (d). ……...37
Figure 26. Suspended particulate matter (mg/L) changes with main depth zones (Surface, mid-depth and near-bottom water) ……...……..38
Figure 27. Suspended particulate matter (mg/L) distribution along distance from the shore (km) (a), and distribution with depth (m) (b)…….....38
Figure 28. Suspended Particulate Matter (mg/L) plotted against chlorophyll-a, showing a linear relationship.. ……...…….....38
Figure 29. Particulate Organic Carbon (µM) (a) and articulate Organic Nitrogen (µM) (b) distribution by depth zones (Surface, mid-depth and near-bottom water)……....39
Figure 30. Particulate Organic Carbon (µM) changes with distance from shore (km) (a), and with depth (m) (b)...…….…….40
Figure 31. Particulate organic nitrogen (µM) distribution along distance from the shore (km) (a), and with depth (m) (b).…….....40
Figure 32. Correlation between particulate organic carbons (µM) and particulate organic nitrogen in the coastal zone of Qatar.…….…….....40
Figure 33. Changes in carbon to nitrogen ratio (C:N) in suspended particulate matter with depth zones (surface, mid-depth and near-bottom water).…….....41
Figure 34. Carbon to Nitrogen ratio (C:N) in suspended particulate matter down distance from shore

(km) (a), and down depth (m) (b)……..….....41
Figure 35. Changes in stable carbon isotope ($\delta^{13}C$) signature with depth zones (Surface, mid-depth and near-bottom water)...……...42
Figure 36. Changes in stable nitrogen isotope ($\delta^{15}N$) signatures with depth zones (surface, mid-depth and near-bottom water) …….43
Figure 37. Stable carbon isotope ($\delta^{13}C$) down depth (m) (a), and down distance from shore (km) (b)……...…….... 43
Figure 38. Stable nitrogen isotope ($\delta^{15}N$) down depth (m) (a), and down distance from shore (km) (b)…….....43
Figure 39. Changes in stable carbon isotope ratios ($\delta^{13}C$) with Temperature (°C) ……..44

LIST OF ABBREVIATIONS:

- BOD : Biological Oxygen Demand
- Chl-a : Chlorophyll-a
- DDW : Distilled Deionized Water
- DIC : Dissolved Inorganic Carbon
- DO : Dissolved Oxygen
- EEZ : Exclusive Economic Zone
- HCl : Hydrochloric Acid
- NH_4^+ : Ammonia
- NO_2^- : Nitrite
- NO_3^- : Nitrate
- PO_4^{3-} : Phosphate
- NED : N-(1-naphthyl)-ethylenediamine
- POC : Particulate Organic Carbon
- POM : Particulate Organic Matter
- PON : Particulate Organic Nitrogen
- PP : Polypropylene
- QA/QC : Quality Assurance/Quality Control
- rpm : Rounds Per Minute
- SiO_4^{2-} : Silicate
- SPM : Suspended Particulate Matter

CHAPTER 1: INTRODUCTION AND LITERATURE REVIEW:

1.1. Introduction:

In marine geochemistry, suspended particulate matters (SPM) play significant roles in several coastal biogeochemical processes including amount of dissolved oxygen available in a water column, transport and bioavailability of contaminants and the amount of carbon sequestration into the sediments (Bizsel et al., 2011). Suspended particulate matters, including suspended particulate organic matter, are ubiquitous, essential and a main component of the marine biogeochemical cycling. Suspended particulate matters contain organic matter (OM) and inorganic fraction that include clay, sand and insoluble minerals (Bizsel et al., 2011). The organic fraction of the SPM (POM) possibly contain a mixture of living microorganisms, non-living matter, and allochthones materials (Chester and Jickells, 2012). The living components is from the plankton (phytoplankton and zooplankton), and the nonliving is from dead organisms as well as fecal matters of these organisms (Chester and Jickells, 2012, Boyd, 2015). Different natural and anthropogenic processes influence the abundance of SPM influence coastal water environment. In fact, the dominant source of organic matter in the ocean is the primary production by photoautotrophs including microalgae, macro-algae and seagrasses (Libes, 2009). Primary production is controlled by array of abiotic factors including nutrients concentrations, light availability and temperature (Valiela, 1995). It is also controlled by biotic factors such as grazing by herbivores, filter feeders and zooplankton (Jenkins, 2001; Chester and Jickells, 2012).

Nutrients, mainly nitrogen and phosphorus, are abio-limiting factors for the primary productivity in ocean environments. Nitrogen gas (N_2) from the atmosphere dissolves in surface water of marine environments, where nitrogen fixing bacteria convert it into a biologically available form as ammonia (NH_3) (Sollai et al, 2015). Other sources of nitrogen to the surface water include river inputs and upwelling from deeper nutrients rich seawater. Because availability of nitrogen for biological productivity is controlled by microbial transformations such as biological fixation, anammox and nitrification-denitrification, nitrogen is a limiting factor for primary productivity in most of the ocean environment (Libes, 2009).

Oceans contain the largest active carbon pool on earth and it exchanges with the atmosphere and cycle in the different pools inside the marine environment through biological, physical and chemical pathways. The three main carbon "pumps" /pathways can be summarized as solubility/physical pump, carbonate pump, and the biological pump. The solubility pump, also known as physical pump, is a physiochemical pathway for atmospheric carbon to enter the marine environments by diffusion through the water-air interface. Another pathway, the carbonate pump, involves precipitation of carbonate, which is in equilibrium with the carbon dioxide in the water that affect the alkalinity of the oceans. A third pathway, the biological fixation of the carbon at the surface of the ocean through the primary production and the export of the produced OM to the deeper ocean remains the major pathway for carbon export in the ocean and is known as the "biological pump" (Sigman and Hain, 2012; Boyd, 2015). This carbon is assimilated into biomass in the photosynthesis and when organisms die, the particles and detritus sink down, thus "pumping" organic carbon towards the bottom of the ocean (Sigman and Hain, 2012; Boyd, 2015, Gupta and McNiel, 2012).

Suspended particulate matters especially the organic matter in the marine environment plays a significant and essential role in the biogeochemical cycles in the oceans, especially the carbon and nitrogen. Understanding the dynamics and composition of SPM is crucial for understanding and predicting several processes the global carbon and nitrogen biogeochemical cycles. Because of their major roles in primary productivity, pollution and in geochemical cycles, monitoring SPM in the coastal water environment is crucial for any coastal management plan and for contributing to understanding the global carbon cycle.

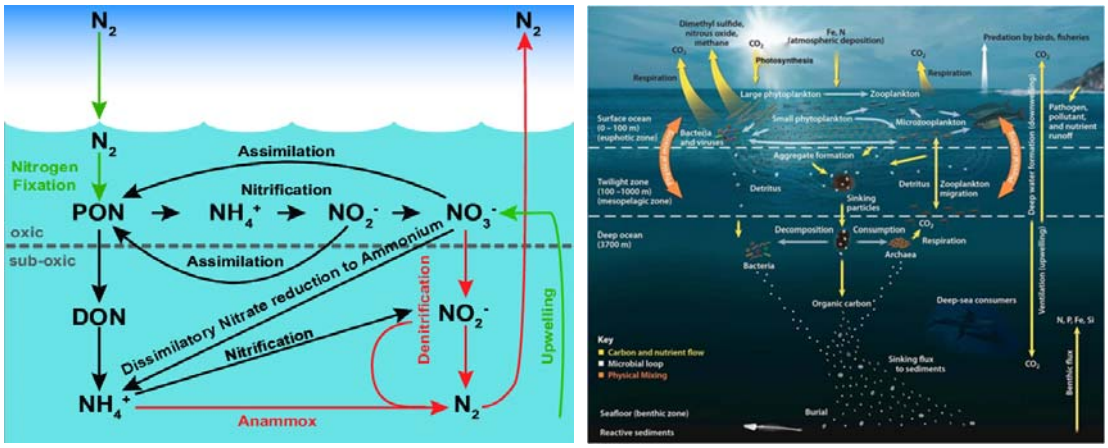

Figure 1. The Oceanic Nitrogen Cycle (left) (Sollai et al, 2015), and the Oceanic Carbon Cycle, showing the complex pathways and forms of carbon that exist in the marine environment, from inorganic to organic, and living to non-living forms of carbon (Oceans and the Carbon Cycle, https://serc.carleton.edu/eslabs/carbon/6a.html)

1.2. Background/Literature Review:

The Arabian Gulf is a shallow, semi-enclosed marginal sea of the Indian Ocean. It is oligotrophic with limited sources of nutrients, mainly nitrogen and phosphorus. Nutrients sources into the Gulf are limited to rivers influx at the very north, exchange with the open ocean through Hormuz at the south and out-welling from coastal habitats. Similarly, inputs of SPM into the Gulf include coastal ecosystems such as mangroves, rivers of the Tigris and Euphrates, and water coming from the Hormuz. The biogeochemistry of the Arabian Gulf is also influenced by introduction of SPM from human related activities such as discharge of domestic wastewater and wastes from different industrial activities. A major source of SPM is the primary production at the surface water. The existing data of chlorophyll and nutrients in the Gulf show that dynamics of chlorophyll and nutrients in the Gulf basin is not fully understood. The nitrogen: phosphorus ratio (N:P) in the waters of the Arabian Gulf are different from the proportion set by Redfield (Al-Yamani and Naqvi, 2018), which indicate impacts of nutrients availability on primary production. Al-Yamani and Naqvi (2018) indicated that the two most impactful key constituents are the reduction of riverine inputs that increasingly cause a rise in salinity of the water, and the large nutrients loading that originates from discharges of sewage waters from the coasts. Although the Arabian Gulf waters are oligotrophic, the sudden

increase of phytoplankton blooms in the past few decades represent an increased risk for eutrophication events in the marine environment. New sources of nitrogen in the ocean are dependent on fractions of influxes from atmosphere through nitrogen fixing microorganisms, from terrestrial coastal inputs onto the marine coastal waters, and from recycling of OM outside the photic zone (Chester and Jickell, 2012). Influxes from sources outside the photic zone usually support new production of organic matter and consequently high formation of detrital matter. Organic matter in seawater is not only originating from autochthonous formation, but it is also influenced by lithogenic and anthropogenic components. The composition of the organic matter is strongly influenced by sources from both marine and terrestrial environment (allochthonous) (Schubert et al, 2001).

Stable carbon and nitrogen isotopes are good tracers for the sources of organic materials. Study of elemental and isotopic composition of stable carbon and nitrogen provide a great indicator of organic matter origin and sources of nutrients in the marine environment. Their use is non-hazardous, with no radiation problems and it is a great and fascinating tool to use for many applications in the study of the marine environment (Hama et al, 1983). Utilizing stable carbon and nitrogen isotopes can be a significant tool for environmental scientists to track source and origin of organic matter in the environment and understand ecosystem trophic dynamics. Stable isotopes are great tracers for comprehension of the flow of energy and the complexity of the food web and trophic structures (Le Vay et al, 2011). During the process of primary production, the primary producers fix carbon (as ^{12}C) and ratios of its stable isotopes (^{13}C and ^{14}C for example). The fixation of carbon as carbon-13 is at a fraction of carbon-12. There are known and certain ratios of carbon ($\delta^{13}C/^{12}C$) and nitrogen ($\delta^{15}N/^{14}N$) and their stable isotopes for different primary producers such as seagrass, mangroves, phytoplankton and macroalgae. For example, mangroves have an average $\delta^{13}C$ of 27.0 ‰ and phytoplankton have averages of 20.0 ‰ (Hughes et al, 1983). There are several factors that controls the fraction of fixed δ15N in the primary producers, mainly plankton. Same factors might also affect the fraction of carbon-13 produced in the marine environment. These factors include abundances of phytoplankton and zooplankton and the amount of nitrate in the surface waters (Libes, 1983). So, it is apparent that stable carbon and nitrogen isotopes are important to fathom the relationships between abundance and production of organic material, primary production and fluxes of nutrients in the marine environment.

There are lack of studies on dynamics of suspended particulate matter, their sources and their

distributions in the marine environment of the Arabian Gulf. Additionally, there are lack of information on the sources of organic matter and sources of nutrients, mainly nitrogen. The use of stable isotopes as tracers and as a tool is very limited in understanding biogeochemical processes in the Arabian Gulf. The applications are limited to mostly terrestrial and geological studies to study history and origin of sediments and the geology in the Arabian Gulf (Chafetz et al, 1994; Holail, 1999 and Holail et al, 2005). There are few applications in marine environmental studies such as in diagenesis of carbonates (Chafetz, et al, 1988) and biota of the coast (Kürten et al, 2014). In Qatar, uses of stable isotopes as tracers in aquatic and marine environmental application are limited to a few studies such as hydrological tracing and investigations into ground water (Yurtsever et al, 1979). The use of carbon and nitrogen stable isotopes in marine environment seems to be limited to two main studies; the first application was on the study of the ecology of feeding in the green tiger shrimp (*Penaeus semisulcates*) in the intertidal and subtidal zones of the waters of Qatar. The study used carbon and nitrogen isotopes to investigate source and types of food that the shrimp consumes. The study of stable isotopes confirmed the role that seagrass beds play in the feeding of juvenile and post larvae of green tiger shrimps (Al-Maslamani et al, 2006). Another study by Walton et al (2016), used δ15N isotope to investigate sources of nutrients in the seagrass beds and possible outwelling in the east coast of Qatar. The study found high variability in the δ15N in a relatively small geographic area. The values measured in March ranged from -12.4 ‰ to +2.94‰, showing a significant variability in δ15N (Walton et al, 2016). The determination of δ15N in the east coast signaled that the seasons and sediment reactions are important influences on the amount of δ15N (Walton et al, 2016). The study recommended that more samples to be collected over space and time in order to understand nutrients dynamics and food sources in the marine environment of Qatar.

The present study will provide a database on concentrations and sources of organic matter in the marine environment of Qatar. It also covers a gap in knowledge on the dynamics of primary production and nutrients in the marine waters at the exclusive economic zone in Qatar. Carbon and Nitrogen stable isotopes will be used to trace sources of organic matter in the Qatari EEZ as well as in identifying sources of nutrients and determining marine primary productivity. The comprehension of the role of stable carbon and nitrogen isotopes as tracers is significant for the determination for oceanic organic matter sources, dynamics of primary production, dynamics of nutrients and in getting a better understanding of the carbon and nitrogen dynamics in the oligotrophic water of the Arabian Gulf. Findings from the present study will enable us

to understand contributions of different sources; such as Tigris and Euphrates River, lateral influx from coastal ecosystems, primary production, among others, to the total organic matter production in the EEZ environment of Qatar.

There are three main research hypotheses in the present study:

1) The amount of Suspended Particulate Matter varies with depth and down distance from the shoreline.
2) The signatures of $\delta^{13}C$ and $\delta^{15}N$ vary with distance from shore and with depth.
3) The Central Arabian Gulf contains different sources of nutrients and is highly influenced by anthropogenic activity.

1.3. Research Objectives:

The objectives of the current study are:

1. To quantify the amount of SPM in three transects in the EEZ of Qatar.
2. To quantify the ratio of stable carbon and nitrogen isotopes in suspended particulate matter
3. To understand the trends of organic matter in the marine environment of Qatar with depth and down distance from shoreline.
4. To understand the effect of different abiotic influences in the central Arabian Gulf on the production of particulate organic matter

1.4. Significance and Reasoning of the Study:

The semi-enclosed marginal sea of the Arabian Gulf receives particulate matter from multiple sources including autochthonous sources from the primary production and allochthones sources including Tigris River in the north, the wetlands across the land-ocean interface, and from the discharge of wastewater. Quantification of the sources and composition of the particulate organic matter in the central Gulf and the environmental forcing behind the existing distribution will be investigated using elemental and isotopic composition of organic matter.

The study enables us to understand the to estimate the contribution of the autochthonous and allochthones organic matter in the carbon budget of the Gulf and potential contribution in the food web as well as in the carbon cycle. The aim of the present study is to quantify the amount of POM in the Central Gulf down three transects crossing the Qatari EEZ. The study will investigate the composition of the OM and its spatial variability in the coastal water of Qatar. The implication of the study in terms of fluxes from the coastal wetlands and/or from the terrestrial environments will be discussed.

CHAPTER 2: STUDY AREA AND BACKGROUND INFORMATION:

The waters of Qatar are located in the central part of the Arabian Gulf. The Gulf is shallow with average depth of 35 m, and a maximum depth of about 100 meters near Iran. The Gulf has high salinity (about 40 PSU) with salinities reaching up to 70 psu at some bays. This salinity extreme is mainly caused by high evaporation (202.6 cm/year) and low precipitation (Al-Ansari et al, 2015). The surface water currents are controlled by the Shamal winds that induces strong currents in the water. The Southwestern part of the Arabian Gulf, around Qatar, receives little precipitation of <5 cm/year (Al-Ansari, 2006).

Figure 2. Map of the hydrography of the Arabian Gulf (Limits in the Seas, 1981).

The coastal areas of the Gulf contain diverse productive ecosystems such as mangroves, seagrass beds and coral reefs (Price et al, 1993; Sheppard, 1992; Nasr, 2014). Phytoplankton primary productivity in the surface water is variable with space and with season, with summer having an apparent increase in the productivity due to optimal conditions (Al-Ansari et al, 2015). Nutrients measurements in the Arabian Gulf are discrete from isolated studies representing small short-term studies with high uncertainties. There is lack of knowledge on the macronutrients dynamics, particulate organic carbon sources and budgets, trends in primary production, and trends of organic matter in the Arabian Gulf. Information on the effects of different stressors such as anthropogenic activities and extreme climatic conditions on the distribution and abundance of organic particulate matter are especially lacking.

CHAPTER 3: MATERIALS AND METHODS:

The sampling was conducted in the Exclusive Economic Zone (EEZ) of Qatar and during late summer (September) of 2019, in three transects crossing the EEZ of Qatar. Sampling, sample processing and *in-situ* measurements for the present study were conducted using the Qatar University's Research Vessel "*RV Janan*". The research vessel is fully equipped with standard oceanography equipment and facilities. These include a wet lab, as well as equipment such as a rosette fitted with 12 Teflon-coated Niskin bottles, sediment grabs, multi-corer and plankton nets. The sampling, sample filtration, sample preservation and storage, and dissolved oxygen analysis, were performed in the vessel's facilities. The analysis for chlorophyll-a and dissolved nutrients (NH_4^+, NO_3^-, NO_2^-, PO_4^{3-} and SiO_4^{2-}), suspended particulate matter (SPM) quantification, and GF/F filter sample processing all conducted in the Chemical Oceanography Lab at the Department of Biological and Environmental Sciences in Qatar University. The suspended particulate matter filter samples were processed and analyzed for stable carbon ($\delta^{13}C$) and nitrogen ($\delta^{15}N$) isotopes, carbon and nitrogen content (%), and the carbon to nitrogen ratio (C:N), at the Stable Isotope Geosciences Facility at Texas A&M University (TAMU), College Station in the United States.

Transects and number of sites per transect were chosen to represent different depths and the different water masses in the waters of Qatar (Figure 4). Sampling locations were chosen to represent vertical and horizontal variabilities in the selected parameters of study (e.g. SPM, chlorophyll, nutrients). Sampling sites included 18 stations (Table 1, Figure 4). The areas of sampling covered diverse topography and waters impacted by waves, currents, and anthropogenic activities.

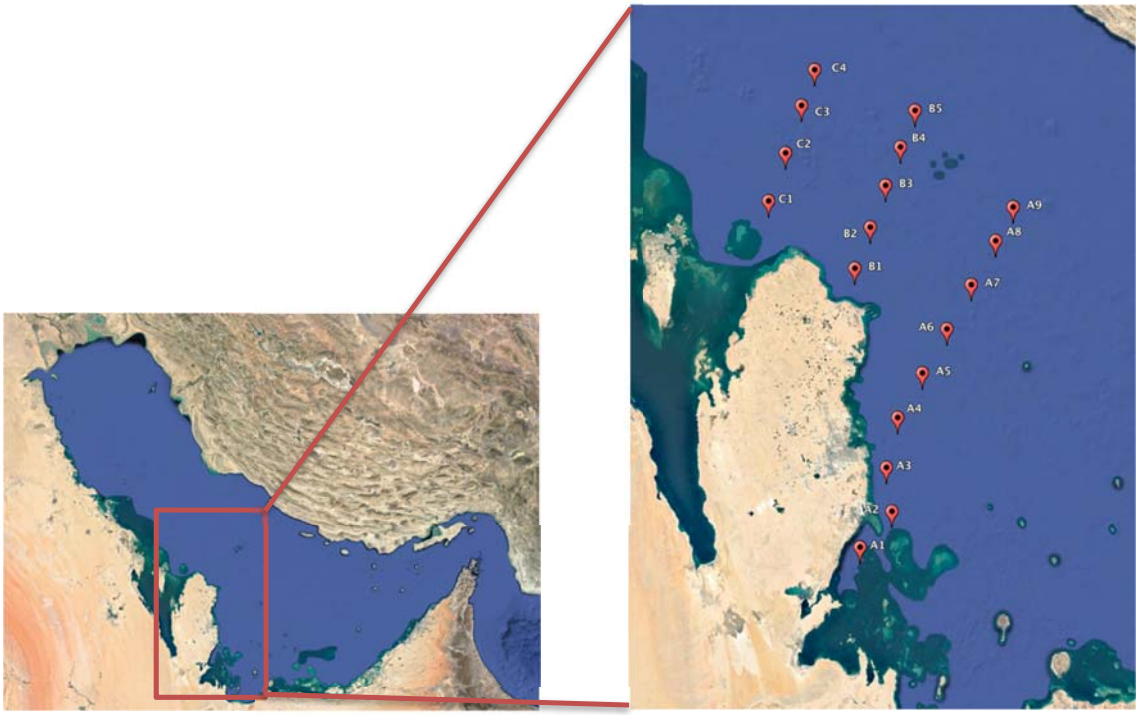

Figure 3. Map of sampling stations in the Exclusive Economic Zone (EEZ), Qatar, in the central Arabian Gulf.

Table 1. Information of eighteen offshore sampling locations within the waters of Qatar's EEZ, including station name/ID, total depth and distance from shore.

Transect #	*Station Name/ID*	*Total Depth [m]*	*Distance from Shore [km]*
A	*A1*	*24.7*	*11.1*
A	*A2*	*36.0*	*17.3*
A	*A3*	*19.1*	*9.7*
A	*A4*	*18.9*	*23.8*
A	*A5*	*24.7*	*40.5*
A	*A6*	*29.4*	*41.8*
A	*A7*	*39.3*	*56.1*
A	*A8*	*50.0*	*75.5*
A	*A9*	*57.9*	*92.1*
B	*B1*	*14.3*	*9.2*
B	*B2*	*24.5*	*31.3*
B	*B3*	*38.6*	*53.8*
B	*B4*	*38.2*	*74.7*
B	*B5*	*69.0*	*94.4*
C	*C1*	*12.6*	*27.9*
C	*C2*	*24.5*	*45.5*
C	*C3*	*24.6*	*67.5*
C	*C4*	*69.0*	*85.9*

3.1. Field Sampling and Samples Processing:

Suspended particulate matters were collected in the late summer of 2019 from 18 locations. Variabilities in concentrations of SPM with depth and distance from shore is determined using standard methods of Levin and Currin (2012), Grasshoff et al (1999), Parsons et al (1984). Carbon and nitrogen stable isotopic ratios of SPM and their molar ratio (C:N) were measured for samples obtained during summer in order to identify their origin. Environmental abiotic parameters including salinity, pH, temperature, fluorescence and nutrients (nitrate, nitrite, phosphate, silicate and ammonia) were all measured using standard methods of Grasshoff et al (1999), Parsons et al (1984), IOC (1993) and Strickland and Parsons (1972). Sampling of seawater for nutrients, chlorophyll and SPM analysis was completed using twelve of 10-liter Teflon-Coated Niskin (Figure 4).

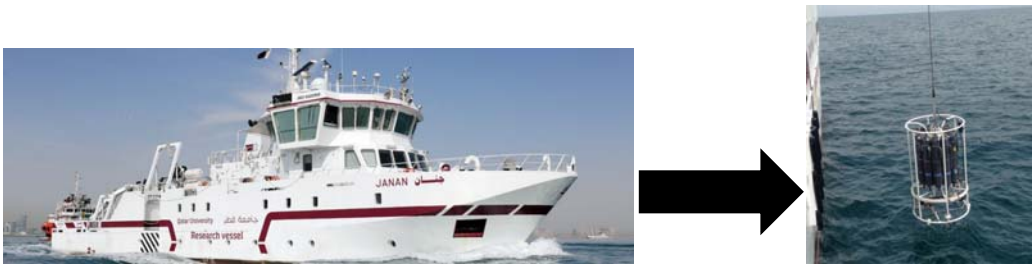

Figure 4. *RV* Janan (left) and the rosette fitted with a dozen Teflon-coated Niskin bottles being lowered onto the water column of the sampling location (right).

3.1.1. Hydrography and Physiochemical Parameters Field Measurements:

Hydrographical parameters are measured in situ using the CTD attached sensor including temperature, salinity, pH, density, fluorescence, dissolved oxygen and oxygen saturation. The hydrographical parameters of the water column at each sampling locations were collected in situ and in continuous reading from the top of the water column to the near bottom (about 50 cm above the ocean floor).

3.1.2. Seawater Dissolved Oxygen (DO):

Seawater dissolved oxygen (DO) in each sampling site/depth was measured manually using the Winkler method. The water samples were collected from the Niskin bottle directly using pre-cleaned 300-mL, Wheaton BOD bottles. A plastic tube is inserted into the Niskin bottle mouth and the other end was inserted into the bottom of the BOD bottle. Extra caution was given to avoid any gas bubbles in the tube, so as not to inject any gases in the sample. The seawater was allowed to overflow from the BOD bottle for approximately 10-15 seconds. Then, the tube was slowly removed from the bottle, ensuring that there is no injection of any air into the sample and interfering with the dissolved oxygen results. The samples were immediately taken for further determination of the dissolved oxygen in the seawater samples.

3.1.3. Nutrients (Nitrate, Nitrite, Phosphate, Silicate and Ammonia):

Dissolved nutrients in seawater samples were collected using Niskin bottles. Seawater was collected in polypropylene (PP) plastic bottles. All the plastic bottles were previously soaked in a 10% HCl acid tank for 24 hours. The bottles were rinsed with DDI water, dried and stored until sampling. Before sampling, the bottles were rinsed with seawater three times. The samples were taken to the wet lab for further analysis. Unfiltered seawater samples were used for the analysis of ammonia to prevent contamination by the filters or atmosphere. Filtered seawater on 0.45 μm Millipore membrane filter samples were used for the analysis of the other nutrients. The filtered seawater was used to avoid uncertainties provided by decomposition as mentioned by Grasshoff et al (1999). Samples were kept frozen at -20 °C in the wet lab onboard the RV, and were transferred to -80 °C freezer upon return to the lab for the analysis.

3.1.4. Suspended Particulate Matter (SPM) and Chlorophyll-a:

Samples for suspended particulate matter (SPM) were collected using Niskin bottles. Samples were filtered on Whatman GF/F filter membranes, with 0.7 μm pore size. The GF/F filters and were weighed on an accurate, sensitive and calibrated analytical balance (Fig. 6). The pre-weighed membrane filters were pre-combusted at 450 °C for four hours as mentioned in the

stable isotope protocol by Levin and Currin (2012) (Fig. 6). The combusted GF/F filters were placed again in clean petri dishes, sealed and stored until sampling (Fig. 6). For QA/QC, the filtration system is cleaned before each sampling and filtration. The flasks of the filtration system were soaked in a 10% HCl acid for 24 hours. The flasks were well rinsed with DDI water and dried.

Figure 5. Preparation of the Whatman GF/F filters by weighing (left), ashing (middle), then labeling and storage of the filters (rigth).

At each sampling site, SPMs were collected at three different water depths. Seawater was determined to be collected at the surface, near-bottom and chlorophyll-maximum depth of the water column at each sampling station. The sampling depths were selected based on real time profiles of hydrography of the water, and mainly fluorescence, verified by the in-situ data obtained during the lowering of the CTD. The fluorescence maximum was used as the proxy for the chlorophyll maximum. Samples of seawater for SPM quantification were obtained from Niskin bottles at each sampling depth. The seawater was pre-filtered using a NITEX mesh screen with a 120-µm mesh size. The funnel and NITEX mesh screen were rinsed at least three times with the filtered seawater. The seawater was pre-filtered to remove the large-sized zooplankton and macro-detrital matter in the seawater according to Levin and Currin (2012). Filtered seawater were collected in a pre-cleaned and rinsed amber glass bottle. During sampling, the Niskin bottles were periodically shaken to prevent the accumulation of particles in the bottom of the bottle and ensure that the seawater sample is homogenous in terms of suspended particles distribution. SPM filtration were conducted using the pre-weighed and pre-combusted GF/F filter membranes. Water sample were filtered in 2-liter intervals, under dim lighting until a rich golden color was obtained on the filter, the filter was almost clogged and the filtration process began to slow down (Fig. 11). The filters were folded, wrapped in aluminum foil and placed in the freezer at -20 °C.

Chlorophyll samples were collected using the same Niskin bottles to collect biomass and SPM to quantify phytoplankton biomass using the pigment chlorophyll-a. Sampling depth were selected based on the same parameters as SPM. About 2 to 5-liter of water were collected from each station in amber glass bottles. All the glass bottles were pre-cleaned by soaking them in 10% hydrochloric acid (HCl) for 24 hours, rinsing with distilled deionized (DDI) water and drying. The filtration was performed on a 0.45 μm, 47 mm, Millipore filter membrane. The filtration was performed under dim light. The filters were wrapped in aluminum foil, labeled and kept frozen at -20 °C. The samples were stored at -80 °C until analysis.

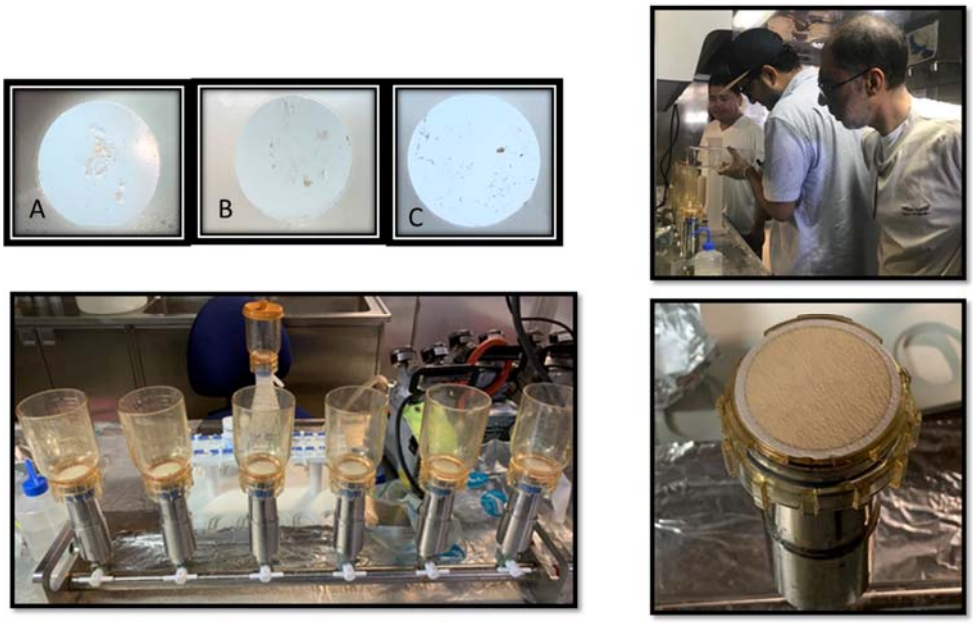

Figure 6. Sampling and pre-filtration and filtration of SPM: the filtrate retained on the NITEX screen (120-μm mesh size) when pre-filtered samples (top left), the pre-cleaned filtration apparatus for the collection of chlorophyll and SPM (bottom left), the filtration of the seawater samples (top left), and SPM retained on the pre-combusted GF/F filter (bottom right).

3.2. Samples processing and analysis:

3.2.1. Dissolved Oxygen (DO):

Laboratory manual analysis for DO was conducted on the *RV* Jenan using Omega Metrohm 888 Titrando system and using Winkler method for dissolved oxygen (1888), with modifications by Strickland and Parsons (1972), Carrit and Carpenter (1966) and Carpenter (1965). Samples were inoculated with 2 mL of manganese (II) chloride and 2 mL of potassium iodide and then 2 mL of 10N sulfuric acid (H_2SO_4) were added. Then, 50 mL of each sample was transferred to a clean 250 mL flask and was titrated with standardized 0.01N thiosulfate solution using starch as indicator. Dissolved oxygen was determined using the following equation:

$$\text{DO } (O_2)\ [\text{mL/L}] = N\ x\ X\ x\ \frac{1000}{V\ x\ {}^{B-4}/_{B}}\ x\ 5.6$$

Where:

N = the normality of sodium thiosulfate
X = volume of titrated sodium thiosulfate in sample
V = volume of the sample (mL)
B = volume of sample bottle (mL)
4 = volume of reagents

And the values added to the equation (except for volume of thiosulfate) were: N = 0.0113, V = 50, and B = 300.

3.2.2. Dissolved Nutrients (NH_4^+, NO_3^-, NO_2^-, PO_4^{3-} and SiO_4^{2-}):

The analysis of the dissolved inorganic nutrients in seawater (NH_4^+, NO_3^-, NO_2^-, PO_4^{3-} and SiO_4^{2-}) were conducted according to the methods of Parsons et al (1984), Strickland and Parsons (1972), IOC (1993) and Grasshoff et al (1999). For the determination of silicate, all preparations and analysis were conducted in plastics. All reagents used in the analysis of the

nutrients in seawater were analytical grade and prepared with double distilled water. For the analysis of ammonia, ammonia-free water was prepared by boiling all double distilled water in the fume hood, and preparing the reagents using this ammonia-free water. Artificial seawater was prepared for their use in determining certain nutrient parameters, more specifically the standards of the said nutrient. The artificial seawater used was prepared according to the expected salinity of the seawater that would be sampled. Therefore, the prepared artificial seawater was with prepared with a salinity of 35 ppt. The analysis of the nutrients was performed using 10-cm cuvette cells on a 6715 UV/Vis Jenway spectrophotometer. Preparation of the standard for each measured nutrients was prepared according to the mentioned methods. For ammonia, ammonium sulfate was chosen as the standard. A stock solution of ammonium sulfate (0.1g NH_4SO_4/ 1000 mL DDW) was prepared, with ammonia-free water. For nitrite, sodium nitrite is used for standard preparation. A stock solution of the standard (0.345g $NaNO_2$ / 1000 mL DDW) was prepared, with a secondary stock solution made with the use of the stock solution (10 mL stock/ 1000 mL DDW), and a third stock (10 mL stock 2/ 100 mL). For nitrate, potassium nitrate was used to prepare a stock solution (1.02g KNO_3/ 1000 mL artificial seawater), with as second stock solution (10 mL stock/ 1000 artificial seawater), and a third stock solution (25 mL of stock 2/ 250 mL artificial seawater). Nitrate standards were made with the use of artificial seawater that's prepared with a salinity of 35 ppt. For phosphate, a standard was prepared using potassium dihydrogen phosphate, which was dried in an oven at 110 ºC until it reached a constant weight. A standard stock was made with a concentration of 10 mmol/L (136.09 mg KH_2PO_4 / 100 mL DDW with 0.2 mL of sulfuric acid). For silicate, a standard was prepared using analytical grade disodium hexafluorosilicate that's been dried in a nickel crucible at 105 ºC in an oven, until constant weight. The standard was made using 188.06 mg Na_2SiF_6/ 100 mL DDW. The stock solution was prepared with a concentration of 10 mmol/L. A secondary standard was prepared with a concentration of 1000 µmol/L (10 mL of stock 1/ 100 mL DDW). A set of 5 concentrations for each nutrient parameter is prepared, twice to determine standard curves for the nutrients. Determination of the standards' concentrations was made using 10-cm cell cuvettes, and 1-cm cells, when needed. Absorbance of the standard was measured at the wavelengths: 640, 543, 880 and 810 nm, for ammonia, nitrite, nitrate, phosphate and silicate, respectively.

Detection limits were determined using the standard deviation of the standard curve values of the blanks for each individual nutrient parameter, calculated as the value of standard deviation value multiplied by 3. Any value determined which is below the detection limit was labeled as

below detection limit (BDL).

The concentrations of the nutrients were measured according to the following equation:

$$Concentration\ of\ nutrient\ parameter = \frac{absorbance\ of\ sample}{slope\ of\ the\ standard\ curve\ of\ nutrient}$$

Table 2. Detection limits for measured nutrients.

Nutrient Parameter	Detection Limit (μM)	N
NH_4^+	0.10	10
NO_2^-	0.01	10
NO_3^-	0.05	10
PO_4^{3-}	0.01	15
SiO_4^{2-}	0.10	10

3.2.2.1. Ammonia (NH_4^+):

Samples for ammonia analysis were thawed, a 50 was used, and 2 mL of phenol reagent (20 g analytical reagent phenol / 200 mL of 95% ethanol) was added and mixed by swirling. Then, 2 mL of sodium nitroprusside solution (1.0g sodium nitroprusside/ 200 mL DDW) was added, followed by 5 mL of oxidizing solution, made with 100 mL of alkaline-citrate solution (100g sodium citrate and 5g sodium hydroxide/ 500 mL DDW) and 25 mL hypochlorite solution (3.5 mL of 1.5N sodium hypochlorite / 100 mL). The samples were mixed gently by swirling between reagent additions. The samples were placed in the dark at room temperature to react for 1 hour. The samples' absorbance were measured in 10 cm cuvettes at the wavelength of 640 nm in the dark, to prevent degradation of the sample's color (IOC, 1993). A reagent blank was made by following same procedure as in the previous samples, but with the use of double distilled, boiled water instead of the sample.

3.2.2.2. Nitrite (NO_2^-):

Samples were thawed and 50 mL was placed in a 250 mL glass reaction flask. Then, 1 mL of the sulfanilamide reagent (5g sulfanilamide/ in 450 mL DDW and 50 mL hydrochloric acid) was added to the samples, then mixed gently by swirling. After 2-10 minutes 1 mL of the NED reagent (0.5g N-(1-naphthyl)-ethylenediamine / 500 mL DDW) is added to the sample, and then mixed. After 10-30 minutes, the absorbance of the samples were measured spectrophotometrically using 10-cm cells at the wavelength of 543 nm. A reagent blank was prepared with the same treatment of the samples, but with double distilled water instead of the seawater samples.

3.2.2.3. Nitrate (NO_3^-):

Before analysis, a cadmium reduction column was prepared for the reduction of the nitrate in the seawater samples to nitrite according to the method of Parsons et al (1984) and IOC (1993). Analytical grade cadmium granules was used, sieved and the fraction of 0.5 to 2.0 millimeters in diameter granules were collected for the column. The cadmium granules were washed with diethyl ether to remove any dirt or grease in the granules (IOC, 1993). Then, they washed with 10N hydrochloric acid, and rinsed with distilled water. Amount of 100 grams was mixed in 500 mL of a 2% w/v copper sulfate solution until the solution's blue color changes. This process was repeated until the color of the copper sulfate solution did not change. A pre-cleaned glass reduction column is prepared by plugging a small glass wool at the bottom of the column, then it was filled with diluted ammonium chloride solution. The cadmium granule slurry were packed into the column carefully, ensuring that there is no air contact. The cadmium reduction column is kept full of dilute ammonium chloride until the sample analysis. Furthermore, the reduction column was periodically tested for efficiency against nitrate standards of known concentrations.

Samples for nitrate analysis were thawed and a 100 mL of each sample was mixed with 2 mL of a concentrated ammonium chloride solution (125g/ 500 mL DDW) and passed through the cadmium column. The first 40 mL of the collected sample was discarded and then the following 50 mL was collected for the analysis. The same procedure of nitrite determination was applied to the reduced samples. A reagent blank is also prepared by using double distilled water and

underwent the exact same process of passing through the reduction column and reagent addition as the samples.

3.2.2.4. Reactive Inorganic Phosphate (PO_4^{3-}):

Samples for phosphate analysis were thawed and mixed with 1 mL of ascorbic acid (10g ascorbic acid in 50 mL DDW and 50 mL of sulfuric acid (4.5 mol/L)). Right after adding ascorbic acid to the sample, 1 mL of the mixed reagent (12.5 g ammonium heptamolybdate tetrahydrate/ 125 mL DDW, 0.5g potassium antimonyl tartrate/ 20 mL DDW, 350 mL of sulfuric acid (4.5 mol/L)) is added to the samples and again mixed in by gently swirling the flask. Sample were left to react for 10 minutes at room temperature. The absorbance of the samples were measured in 10 cm cells at the wavelength of 880 nm within 10 to 30 minutes. The reagent blank was prepared the same manner as the samples, but with double distilled water instead of the seawater samples.

3.2.2.5. Dissolved Inorganic Reactive Silicate (SiO_4^{2-}):

Samples for silicate analysis were thawed and 2 mL of the acid-molybdate reagent (38 g ammonium heptamolybdate tetrahydrate/ 300 mL DDW, 300 mL sulfuric acid (4.5 mol/L)) was added to a 50 mL of each sample. The solution was left for 5 to 10 minutes to react. Then, 2 mL of oxalic acid (10 g oxalic acid/ 100 DDW) was added followed by 1 mL of the ascorbic acid (2.8 g ascorbic acid/ 100 mL DDW), and after mixing, samples were left for 30 -60 minutes and then the absorbance for each sample was measured in a 10 cm cell at the wavelength of 810 nm. A reagent blank wa prepared with double distilled water, with all reagents added and undergoing the same steps of analysis as the samples.

3.2.3. Chlorophyll-a:

Chlorophyll-a (Chl-a) concentration was usually used as a proxy for the amount of photosynthetic pigments in seawater samples (Biomass) (Parsons et al, 1984). The standard Chl-a extraction method using 90% acetone was used according to by Parsons et al (1984), Strickland and Parsons (1972), Jeffrey and Humphrey (1975). The method's detection limit

was 0.006 mg/m^3, which was determined by measuring the absorbance of 3 blanks and calculating their standard deviation. The Chl-a filter papers were extracted with 10 mL of 90% acetone, shaken vigorously, covered with aluminum foil and placed in the refrigerator overnight (~12-16 hours). The solution was centrifuged at 4500 rpm for 10 minutes. Samples were analyzed using 1-cm cell on 6715 UV/Vis Jenway spectrophotometer, and using 90% acetone as the blank, in the dim lighting. Absorbance of the samples was measured at the wavelengths of 750, 664, 547 and 630 nm.

The concentrations of chlorophyll-a were calculated according to Parsons et al. (1984), Jeffrey and Humphrey (1975) and Strickland and Parsons (1972), using the equation:

$$\text{Chlorophyll-a} = 11.85\ E_{664} - 1.54\ E_{647} - 0.08\ E_{630} \quad (\textit{equation 1})$$

With E standing for the absorbance at the measured wavelengths and corrected for the 750 nm readings by subtracting all the values of the other wavelengths from the 750 nm reading. The chlorophyll-a concentration of each sample was calculated by using the equation:

$$\frac{C\ x\ v}{V\ x\ l} = \text{mg/m}^3 \text{ of chlorophyll-a} \quad (\textit{equation 2})$$

Where:

C = the chlorophyll value calculated in equation 1
v = volume of acetone used (mL)
l = the length of the cell used
V = volume of the filtered seawater (L)

And the values of the equation to calculate chlorophyll-a are as follows: V = 2 liters, v = 15 mL and l = 1 cm.

3.2.4. SPM Nitrogen and Carbon Stable Isotopes:

The GF/F membrane filters were thawed and placed on a clean foil for drying to measure dry weight of SPM samples. Filters were dried in an oven at 65 °C for 24 hours and dried completely to a constant weight. Samples are weighed on an analytical balance to quantify the weight of suspended matter on the filters. Samples were then placed in aluminum foil and in pre-combusted glass jars. Samples were analyzed in the Stable Isotope Geosciences Facility in Texas A&M University, College Station. The GF/F filters were placed in tin capsules. Analysis was performed using a Thermo Scientific Flash EA Isolink Elemental Analyze, attached to a Thermo Scientific Conflo IV and a Thermo Scientific Delta V Advantage Isotope Ratio Mass Spectrometer (IRMS). Samples were combusted with pure oxygen at a temperature of 1020°C. Combusted samples were passed through a chromium and cobalt reactor bed, which oxidize the gases produced by the combusted samples. The produced gases were passed through a secondary reduction reactor bed, which has been filled with copper wire, and kept there at a temperature of 650°C. This step was very important for the nitrogen oxides produced in the first reactor to be reduced to nitrogen gas, to be analyzed in the isotope ratio mass spectrometer. Moreover, the water that was produced by the sample combustion was trapped in an anhydrous magnesium perchlorate in-line bed. Subsequently, sample gases were determined and separated, chromatographically, at 55°C before insertion to the Conflo IV and introduction to the Isotope ratio Mass Spectrometer.

The peak areas of the mass-to-charge ratios (28 for nitrogen gas and 44 for carbon dioxide) of the combusted samples were converted to total mass of carbon and nitrogen, which was completed using an intra-run calibration. This calibration was conducted with a methionine standard that was prepared in 5 different masses at the range of 0.05 – 1.5 mg, respectively. The peak areas of the analysis of the standard is regressed against the identified amount of carbon and nitrogen that is in the prepared standards' (methionine) masses, which have been used in the calibration, with a highly linear relationship. The calibration was applied to the peak areas of the samples that were analyzed, to allow for determination of the total carbon and nitrogen content of the samples. The samples' raw $\delta^{13}C$ and $\delta^{15}N$ values were converted to the Vienna Pee Dee Belemnite (VPDB) and Air isotopic scales. This was done by an intra-run, two-point calibration of standards of L-glutamic acid (approximately 1 mg), that have known isotopic values. The standards of L-glutamic acid used were USGS 40 and USGS 41, which had the values of $\delta^{15}N$ = -4.52‰ Air, $\delta^{13}C$ = -26.39‰ VPDB (USGS 40), and $\delta^{15}N$ = 47.57‰

Air, $\delta^{13}C$ = 37.63‰ VPDB (USGS 41), respectively. Internal lab standards were used to perform tests for precision and accuracy of the calibrations, all of which have at least one with a matrix similar to the calibrations. The known values of the internal standard have an uncertainty of ±0.2‰ for both $\delta^{15}N$ and $\delta^{13}C$, respectively. The internal lab standards and their isotopic values were: pure crystalline acetanilide ($\delta^{15}N$ = 0.2‰ Air, $\delta^{13}C$ = -30.2‰ VPDB), powdered, decarbonated sediment standard ($\delta^{15}N$ = 5.2‰ Air, $\delta^{13}C$ = -26.4‰ VPDB), and homogenized, powdered rice ($\delta^{15}N$ = 1.0‰ Air, $\delta^{13}C$ = -29.1‰ VPDB).

The isotopic values are determined using the equations:

$$\delta^{13}C\ (‰) = \frac{\frac{13C}{12C} of\ sample}{\frac{13C}{12C} of\ standard} \text{ -1 x 1000}$$

$$\delta^{15}N\ (‰) = \frac{\frac{15N}{13N} of\ sample}{\frac{15N}{13N} of\ standard} \text{ -1 x 1000}$$

Particulate organic carbon and nitrogen have been determined by taking the total carbon and nitrogen of the sample, reported in (mg), and using the following equations:

$$C\ (\mu M) = \frac{(S-B)\ x\ 1000}{V\ x\ C}$$

$$N\ (\mu M) = \frac{(S-B)\ x\ 1000}{V\ x\ N}$$

Where:

S = sample corrected for the % of combusted sample (mg)

B = tin blank (mg)

V = Volume of seawater filtered

And C and N stand for the standard atomic weight of carbon and nitrogen, respectively. Carbon to Nitrogen ratio was determined by dividing the amount of carbon (mg) over the amount of nitrogen (mg) to get the ratio between both in a sample.

Figure 7. SPM on GF/F membrane filter. Sample were dried at 60 °C, placed in labeled, aluminum foil tubes in a pre-combusted glass jars.

3.2.5. Analysis of Data and Graphical Techniques:

Data were analyzed using univariate and graphical techniques of SPSS software. The Analysis of Variance (ANOVA) and Univariate techniques were used to test for spatial and temporal variabilities in SPM and Chl-a. Correlation and regression analysis was used to test for the effects of environmental parameters on levels and distribution of SPM, chlorophyll, nutrients and stable isotopes.

CHAPTER 4: RESULTS

4.1. Hydrography and physiochemical parameters:

Water temperature varied in the sampling stations ranged between 25.13 to 34.61 °C, with an average temperature of 31.38± 3.29 °C (Table 3). The highest temperatures were recorded at the A4, A5 and A6, at the surface waters, with temperatures of 34.16, 34.61 and 34.06 °C, respectively. On the other hand, the lowest temperatures were recorded at the deepest stations' near bottom sampling sites of A9, B5 and C4, with temperatures of 23.97, 21.92 and 22.91 °C respectively. Water temperatures generally decreased with sampling depths (Figure 8, b). Temperature showed a significant linear decrease with depth (R^2= 0.54, $p<0.01$).

Salinity was generally higher in the south than in the north. Data from the study showed a significant longitudinal decrease of surface water salinity from the southern region (station A1) towards the northern region (station A9) of the EEZ of Qatar, with a range of 45.37 psu (station A1) to 39.44 psu (station A9). Generally, seawater salinity ranged between 38.33 to 46.40 ± 3.29 psu (Table 3). The average salinity was 40.66 psu. Salinity showed minor variabilities with depths (40.32 – 41.14 psu). Salinity showed slight increase with depth however this change was insignificant ($P>0.05$). The highest salinity was recorded at station A1 at all depths of the water column, with salinity values of 45.37, 45.89 and 46.60 psu, respectively. Meanwhile, the lowest recoded values of salinity were found to be at stations B4, B2 and A8, at the surface depth of the water column, with salinities of 38.33, 39.03 and 39.21 psu.

Seawater pH ranged between 7.93 and 8.32, with an average of 8.16± 0.12. The pH showed a decrease with increasing water depth (Figure 19, b). The pH of seawater was highest at stations A9 and A8 at the surface of the water column, with pH values of 8.32 and 8.31 respectively. Seawater pH was at its lowest at station A1, with values between 7.97 – 7.93. Furthermore, the seawater pH showed a longitudinal increase from the south to north of the EEZ, with a slight increase from station A4 to A9.

Seawater density ranged between 22.76 and 30.59 (sigma-theta), with an average of 25.45 (sigma-theta). The density of the water column (sigma theta) increased with depth. The highest seawater density was found at station A1, with highest density at the mid-depth and near bottom waters with values of 30.28 and 30.59 (sigma-theta). On the contrary, the lowest seawater

density were detected in stations B3 and B4, at the surface of the water, with values of 22.87 and 22.76 (sigma-theta), respectively. Additionally, seawater density showed a longitudinal decrease from the south to the north of the EEZ (at the surface of the water column, with a steady increase in density going toward the deepest stations, towards the north of the EEZ (A9). Different water masses in the Gulf region were identified by plotting the T-S diagram (Figure 8, a and b). It is apparent that Sites A4, A5 and A6 were having the highest salinity (≥ 42 psu). These locations represent the shallowest southern region in the east coast of Qatar. C1. C2, A6 are sites of salinity (> 40 psu) and high temperature (>35 °C). Stations C4, B5, A9 represent the most distant sites of all transects with salinities (>40) and low temperature. Surface water showed the highest temperature while the near bottom water showed temperatures close to 20 °C, especially for the offshore sites (Figure. 8, b).

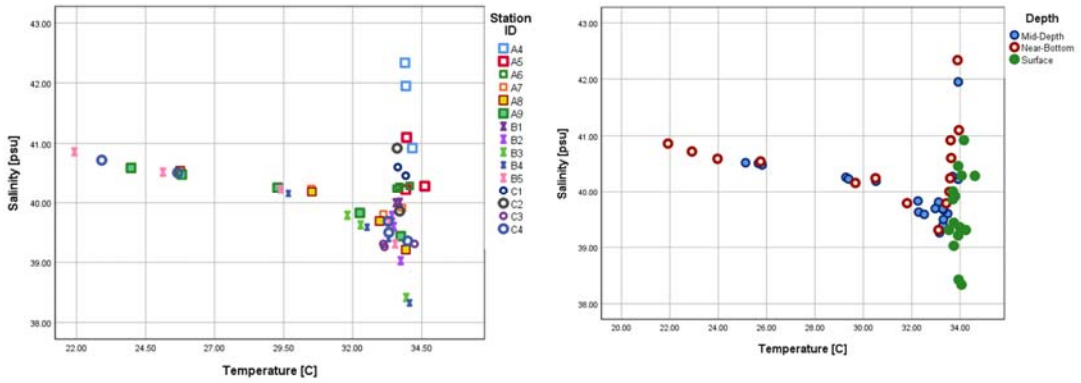

(a) (b)

Figure 8. Temperature-Salinity plots by sample (a) and by depth (b), showing different water masses in the EEZ of Qatar.

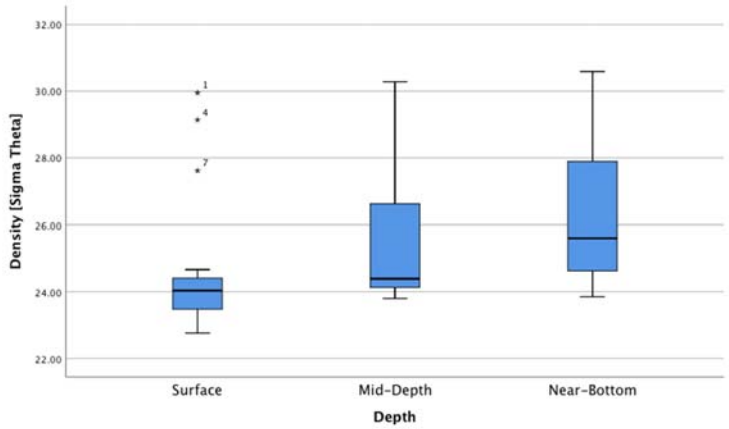

Figure 9. Density (σt) in three main sampling depth zones (surface, mid-depth and near bottom water).

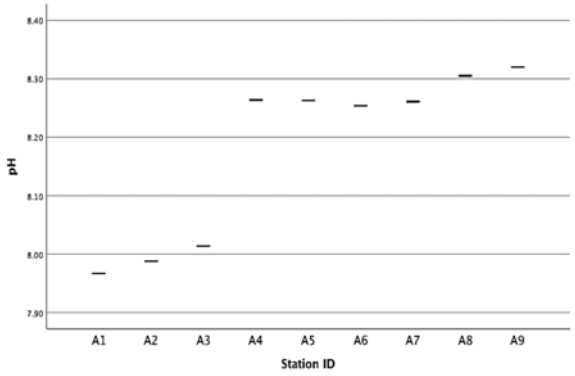

Figure 10. Seawater pH down transect "A" extending from south to north of EEZ, showing an increase from the south (A1) to north (A9).

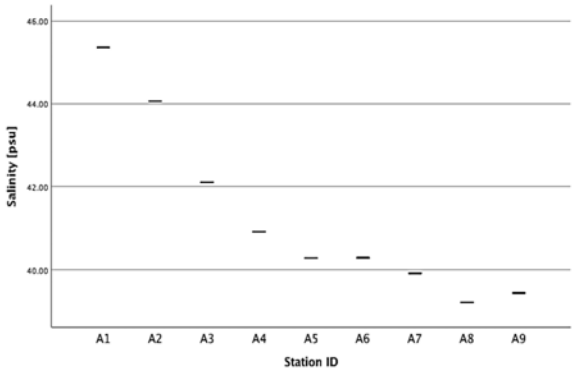

Figure 11. Surface salinity (psu) of seawater down transect "A" extending from south to north of EEZ, showing a clear decrease in salinity from the south (A1) to north (A9).

4.2. Dissolved Oxygen:

Dissolved oxygen (DO) showed significant variation with depth and down distance from shore ($P< 0.05$). Dissolved oxygen ranged between 1.18 and 4.87 ml/L, with a mean concentration of 3.15 ± 1.02 ml/L. Dissolved oxygen was highest at the surface, and lowest at the mid-depth region, with a slight increase at the bottom (Figure 16). It was highest at the surface of the stations A1 and A7, with concentrations of 4.76 and 4.78 ml/L, respectively. Meanwhile, the lowest concentrations of dissolved oxygen were found at the stations B5, B4 and B3 with concentrations of 1.37, 1.18 and 1.37 ml/L, respectively. The lowest DO concentrations were reported from stations B5 and B3 at the most distant mid-depth sites, and at the near bottom water of B4.

Dissolved oxygen (DO) showed a linear decrease with depth (Figure 16), (R^2 =0.51, $p <0.01$). An apparent abrupt change in dissolved oxygen from 4.8 to 1.18 ml/L was prominent mainly at the offshore locations, with the greatest decline at the near-bottom water. Similarly, dissolved oxygen showed a significant decrease with increasing distance from the shoreline (R^2= 0.35, $p< 0.01$) (Figure 13, b).

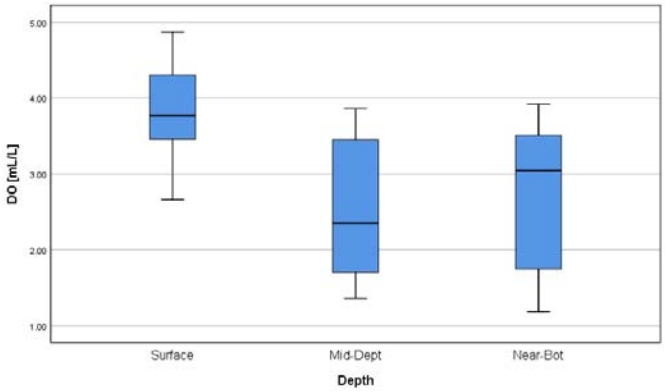

Figure 12. Change in dissolved oxygen (DO) in in the study area (mL/L) with depth (surface, mid-depth and near-bottom water).

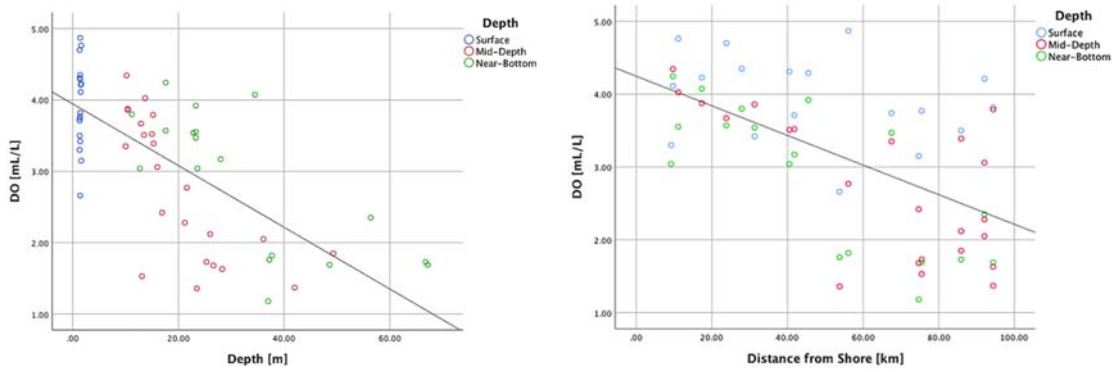

(a) (b)

Figure 13. Change of dissolved oxygen (DO) (mL/L) with depth (m) (left) and with distance from shore (right).

Table 3. Summary of range and mean values of temperature, salinity, pH, density, dissolved oxygen, and oxygen saturation in the Exclusive Economic Zone (EEZ) of Qatar. The data is for the summer season (September 2019):

	Depth					
Hydrographic Parameter	Surface (1.3-1.6 m)	Depth range-1 (10.0-23.5 m)	Depth range-2 (21.2-28.3 m)	Depth range-3 (36.1-49.3 m)	Near-Bottom (12.7-67.2 m)	All
Temp. [°C]						
Minimum	28.78	28.29	29.28	25.13	21.92	25.13
Maximum	34.61	33.69	33.29	25.81	33.95	34.61
Mean	33.03	32.29	31.00	25.53	30.06	31.38
STD	2.11	2.01	1.83	0.36	4.09	3.29
Salinity [ppt]						
Minimum	38.33	39.26	39.59	40.48	39.31	38.33
Maximum	45.37	45.89	40.26	40.52	46.40	46.40
Mean	40.32	40.74	39.99	40.51	41.14	40.66
STD	1.84	1.98	0.32	0.02	1.79	1.74

Table 4. Summary of range and mean values of pH and density in the Exclusive Economic Zone (EEZ) of Qatar in the late summer of 2019, (September 2019):

	Depth					
Hydrographic Parameter	Surface (1.3-1.6 m)	Depth range (10.0-23.5 m)	Depth range (21.2-28.3 m)	Depth range (36.1-49.3 m)	Near-Bottom (12.7-67.2 m)	All
pH						
Minimum	7.97	7.95	8.05	8.04	7.93	7.93
Maximum	8.32	8.29	8.26	8.07	8.25	8.32
Mean	8.22	8.18	8.10	8.06	8.11	8.16
STD	0.11	0.12	0.09	0.02	0.11	0.12
Density [σt]						
Minimum	22.76	23.8	24.07	27.24	23.85	22.76
Maximum	29.95	30.28	26.00	27.48	30.59	30.59
Mean	24.62	25.20	25.13	27.34	26.26	25.45
STD	2.07	2.10	0.90	0.13	2.09	2.07

4.3. Nutrients (nitrate, nitrite, phosphate, silicate and ammonia):

4.3.1. Ammonia:

Ammonia in the study area showed a slight increase at the mid-depth zone, however the variability with depth was not significant ($P<0.05$), (Fig. 14). Ammonia in the study area ranged between 0.14 – 5.24 ± 1.33 (µmol/L), with a mean value of 1.83 ± 1.33 µmol/L. Ammonia had the highest concentrations at the surface of the B5 and C4 stations, with concentrations of 4.66, 5.34 and 4.16 µmol/L, respectively. Meanwhile, the lowest dissolved ammonia concentration was found at the stations A9, B1, C1 (0.18, 0.14 and 0.14 µmol/L, respectively). The ammonia showed an inverted parabolic trend with distance from shoreline ($R^2= 0.21$, $p<0.01$), with lowest concentrations at mid-distance from shoreline.

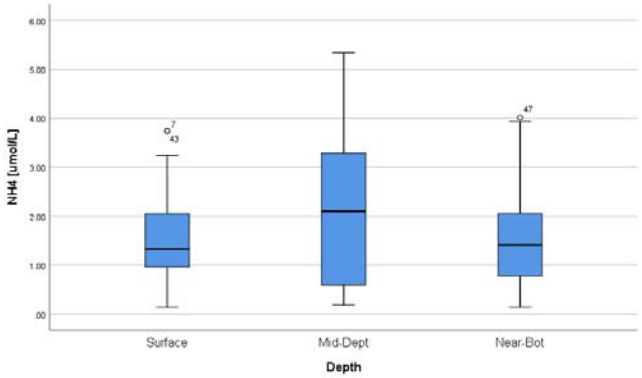

Figure 14. Dissolved Ammonia (NH_4^+) in seawater (µM) with depth as surface, mid-depth and near-bottom water.

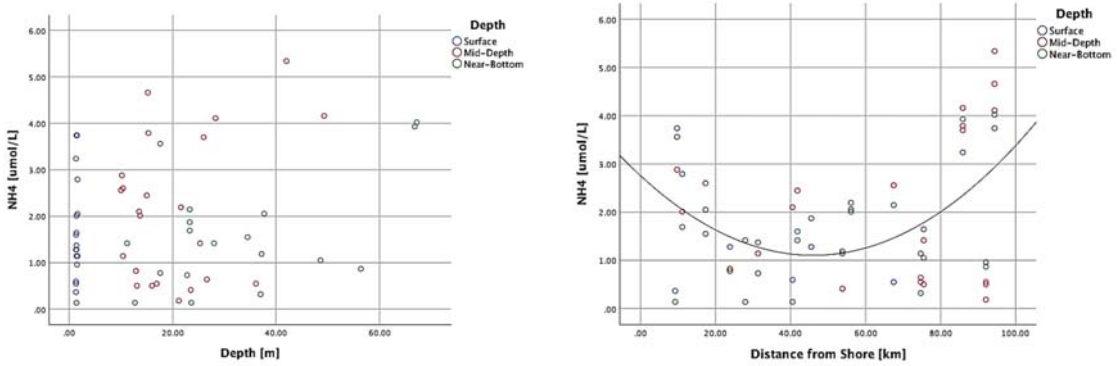

(a) (b)

Figure 15. Dissolved Ammonia (NH_4^+) in seawater (µmol/L) with depth (m), with no discernable trend (a), and along distance from shore (km) (b).

4.3.2. Nitrate:

Nitrate ranged between 0.10 – 9.64 ± 2.76 µmol/L, with an average value of 1.98 µmol/L. The nitrate concentration was highest at the bottom of the offshore stations (A9, B5, and C4), with concentrations of 7.96, 8.02 and 9.64 µmol/L, respectively. The lowest nitrate concentrations were found at the surface water with lowest levels reported at A8, B2, B5 and C4 (0.14, 0.12, 0.10, and 0.15 µmol/L, respectively). Nitrate showed a significant linear increase with depth (R2= 0.75, $p<0.01$) (Figure 17, a). Nitrate showed a general exponential increase with distance from shore ($R^2 = 0.3$, $p <0.01$).

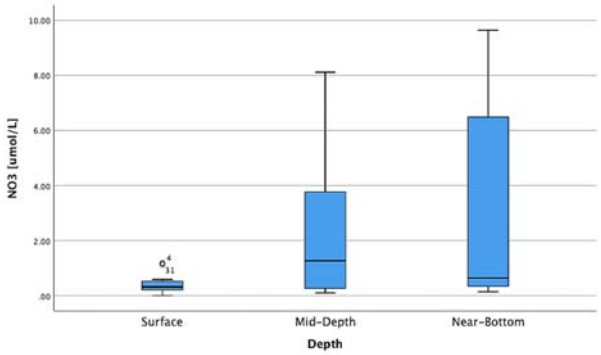

Figure 16. Dissolved Nitrate (NO_3^-) in Seawater (µM) with depth zone in surface, mid-depth and near-bottom water.

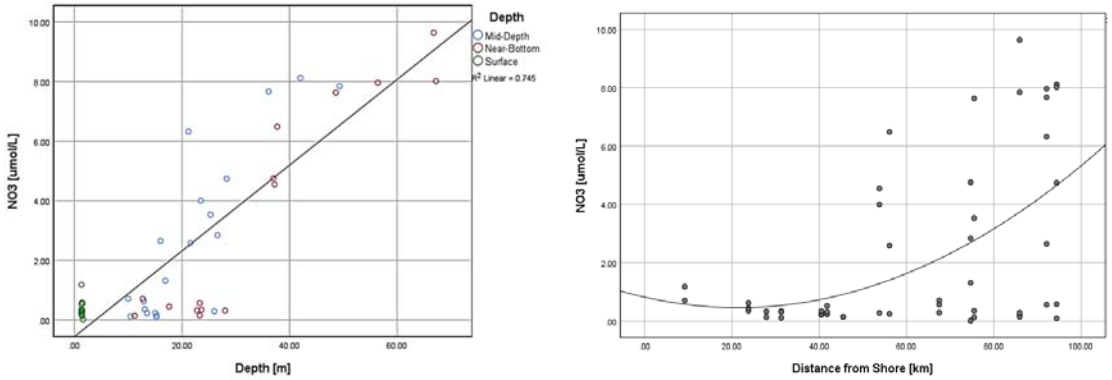

(a) (b)

Figure 17. Dissolved Nitrate (NO_3^-) in Seawater (µmol/L) plotted with depth (m) (a), and with distance from shore (km) (b).

4.3.3. Nitrite:

Nitrite in the study region during the summer of 2019 ranged between 0.13 and 2.02 µmol/L, with an average value of 0.25± 0.42 µmol/L. Nitrite concentration was highest near the bottom and mid-depths of the stations B3 and B4 (1.84, 2.02 and 1,13 µmol/L, respectively). The lowest amounts of nitrite were found in A6, A8, C4 and B5 (0.02, 0.04, 0.05 and 0.06 µmol/L, respectively). Nitrite showed a parabolic trend with depth with highest levels at mid-depth (Figures 18 and 19, a), (R^2 = 0.3, p <0.01). Nitrite concentrations were also higher at the offshore water (R^2 = 0.13, p <0.05).

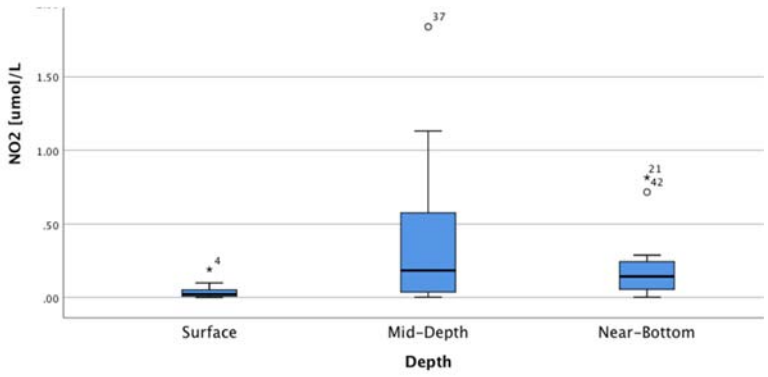

Figure 18. Change in dissolved Nitrite (NO_2^-) in Seawater (µM) with three main depths, (surface, mid-depth and near-bottom sampling depth).

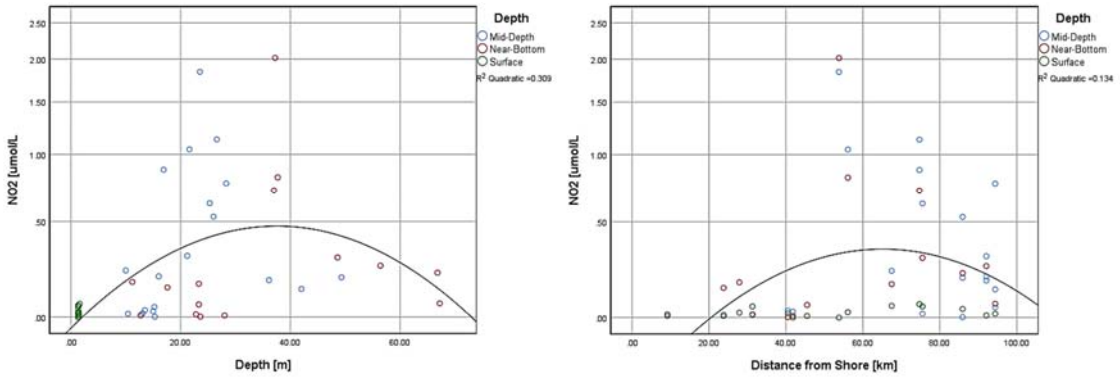

(a) (b)

Figure 19. Dissolved Nitrite (NO_2^-) in Seawater (µmol/L) plotted with depth (m) (a), and with distance from shore (km), showing a quadratic trend (b).

4.3.4. Phosphate:

Phosphate in the study area ranged between 0.07 and 0.65 µmol/L, with a mean value of 0.14± 0.20. The highest PO_4^{3-} concentrations were recorded in the deeper water/near-bottom of stations A9, B5 and C4 (0.60, 0.65 and 0.55 µmol/L respectively. The lowest Phosphate (PO_4^{3-}) concentrations were found at the shallow locations of A2, A6, B2 and C1 with concentrations of 0.02, 0.04, 0.03 and 0.04 µmol/L, respectively. Phosphate was at its lowest at the surface water then it generally increased with increasing depth (Figure 21, a). Phosphate showed a

significant linear increase with the depth ($R^2 = 0.74$, $p < 0.01$). On the other hand, phosphate concentration showed a linear increase with distance from shore ($R^2 = 0.30$, $p < 0.01$), (Figure 21, b).

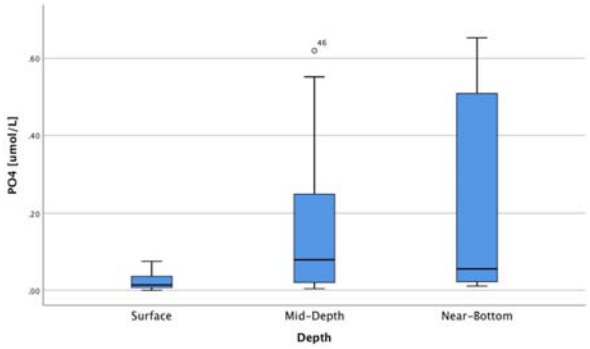

Figure 20. Dissolved Phosphate (PO_4^{3-}) in Seawater (µM) with three main depth zones (surface, mid-depth and near-bottom water).

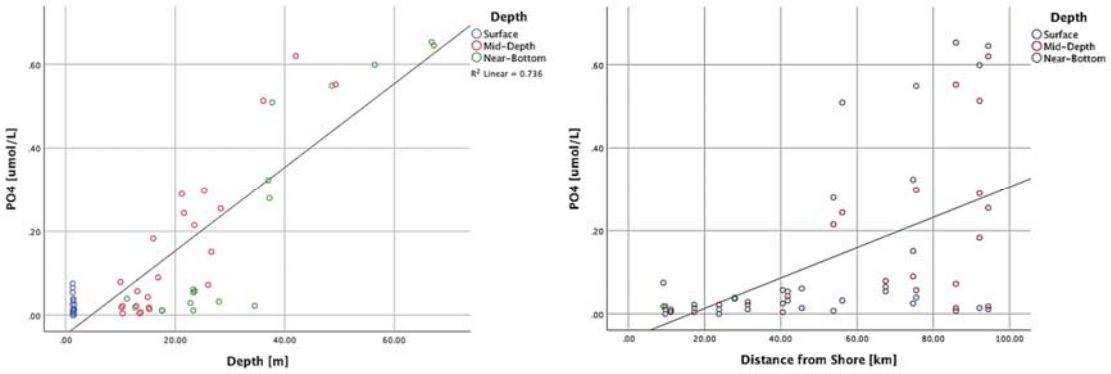

(a) (b)

Figure 21. Dissolved Phosphate (PO_4^{-3}) in Seawater (umol/L) plotted with depth (m) (a), and with distance from shore (km) (b).

4.3.5. Silicate:

Silicate in the study area ranged between 0.16 - 14.86 ± 3.30 µmol/L, with an average concentration of 2.88 µmol/L. Silicate concentration was lowest at the surface but the highest concentration was found near the bottom water (Figure 23, b), especially in the offshore location. The highest concentrations of silicate were found at A7, A8, B5 and C4 (12.14, 9.08, 14.86 and 10.12 µmol/L, respectively), with the highest concentration at the near-bottom of

station B5 (Figures 22 and 23, a). The lowest concentrations of silicate were found at the mid-depth of the offshore locations and some shallow locations at A3, A5, A6 and A9 (0.17, 0.18, 0.16 and 0.17 µmol/L respectively) (Figure 23, b). Silicate showed a significant linear relation with depth (R^2 = 0.6, $p<0.01$), (Figure 23, a). However, silicate didn't show any significant relationship with distance from shore (Figure 23, b).

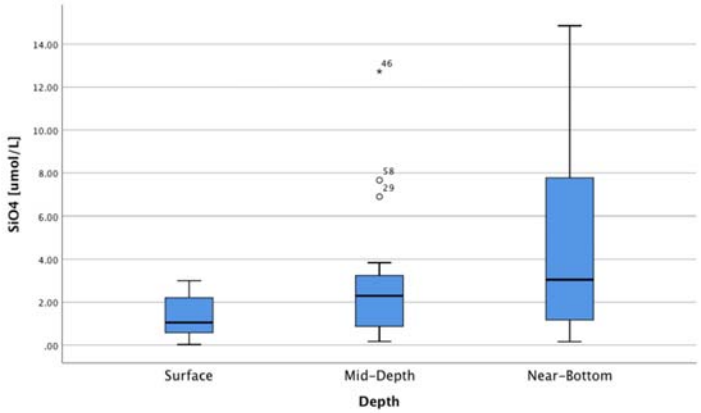

Figure 22. Dissolved Silicate (SiO_4^{2-}) in Seawater (µM) in three main depth zones (surface, mid-depth and near-bottom water).

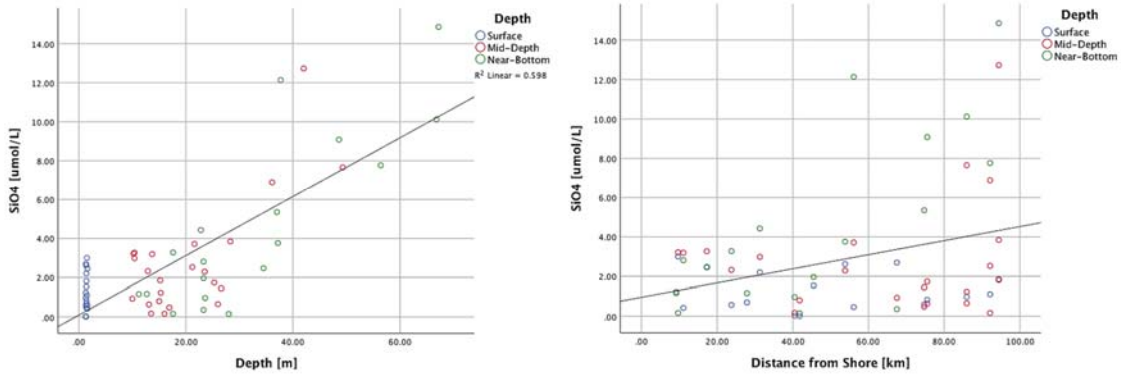

(a) (b)

Figure 23. Dissolved Silicate (SiO_4^{-2}) in Seawater (µmol/L) changes with depth (m) (a), and with distance from shore (km) (b).

4.4. Chlorophyll-a:

Chlorophyll-a concentration ranged between 0.08 and 2.13 mg/m^3 with a mean concentration of 0.76 ± 0.42 mg/m^3. Chlorophyll-a was found to be highest at the middle depths and near the

bottom of stations A4, A5 and B2, with concentrations of 1.80, 1.63, 1.86 and 2.13 mg/m3. The highest chlorophyll-a concentration was found at B2 (2.13 mg/m^3). Meanwhile, stations A9, B5 and C4 had the lowest amounts of chlorophyll-a recorded (0.08, 0.08 and 0.09 mg/m3, respectively). These values were recorded at the bottom of the three furthest sampling stations (Figure 4), at depths exceeding 50 meters. The chlorophyll-a showed a maximum around 20 m depth with and a general decrease at the deeper water. Chlorophyll-a showed a peak at a depth range between 10-30 m, and then a general decrease in the near bottom water (R^2 =0.35, p>0.01) (Figure 24, b). Chlorophyll-a showed a general significant decrease with distance from shore (R^2 = 0.35, p>0.01) with a general peak in concentrations within 20-40 km from the shore line and then a general decrease beyond this zone. (Figure 24, a).

Chlorophyll-a showed significant changes with changes in selected nutrients including nitrate, phosphate and silicate. Chlorophyll-a exponentially decreased with increasing nitrate (R^2 = 0.34, p<0.01), phosphate (R^2 = 0.35, p <0.01) and silicate (R^2 = 0.34, p<0.01), respectively (Figure 25, a, b and c). Chlorophyll-a also showed a significant increase with increasing water temperature (R^2 = 0.51 and p<0.01). (Figure 25, d).

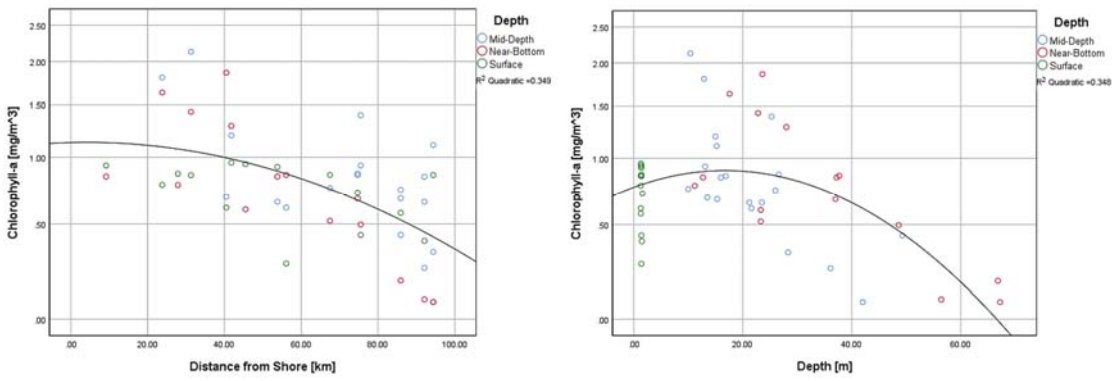

(a) (b)

Figure 24. Chlorophyll-a (mg/m^3) concentration with distance from shore (km) (a), and with depth (m) (b).

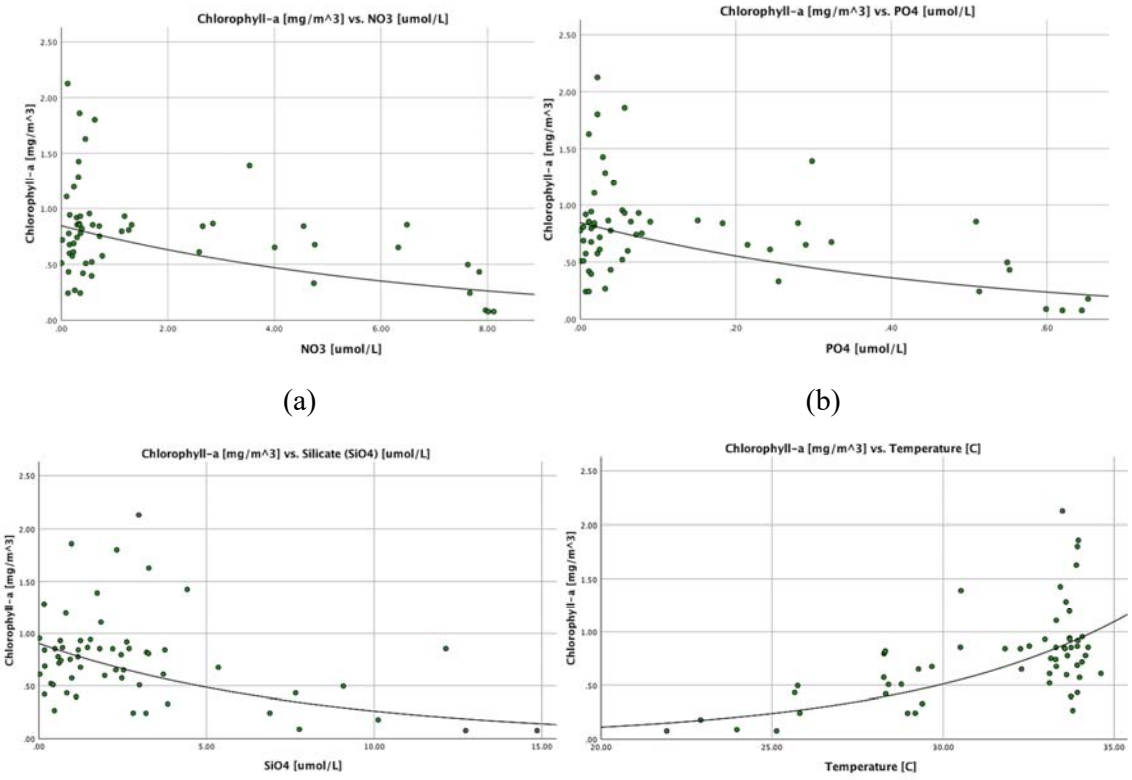

Figure 25. Changes in chlorophyll-a (mg/m^3) concentrations with nitrate (NO_3^-) (µmol/L) (a), phosphate (PO_4^{-3}) (µmol/L) (b), silicate (SiO_4^{-2}) (µmol/L) (c), and temperature (°C) (d).

4.5. Suspended particulate matter and stable isotopes of carbon and nitrogen:

4.5.1. Suspended particulate matter (SPM):

SPM varied significantly between stations ($P<0.05$) and ranged between (3.67 – 19.20 mg/L) with a mean value of 8.76 ± 3.71 (mg/L). Suspended particulate matter was found to be highest at depths range between 21.2 – 49.3 meters, and was lowest at the depth range of 21 -28.3 meters (Figure 27, b). Suspended particulate matter showed a general exponential decrease with distance from shore ($R^2 = 0.5$, $p < 0.01$). Chlorophyll-a was a significant component of SPM ($R^2 = 0.3$, $p < 0.00$) but the majority of SPM was of other sources.

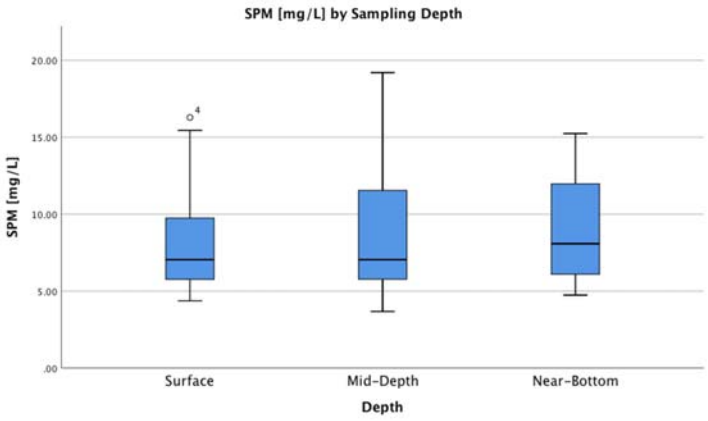

Figure 26. Suspended particulate matter (mg/L) changes with main depth zones (Surface, mid-depth and near-bottom water).

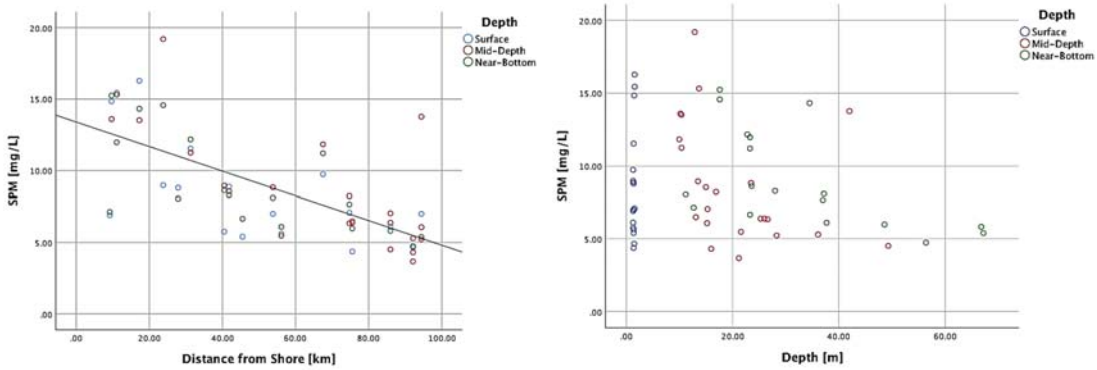

(a) (b)

Figure 27. Suspended particulate matter (mg/L) distribution along distance from the shore (km) (a), and distribution with depth (m) (b).

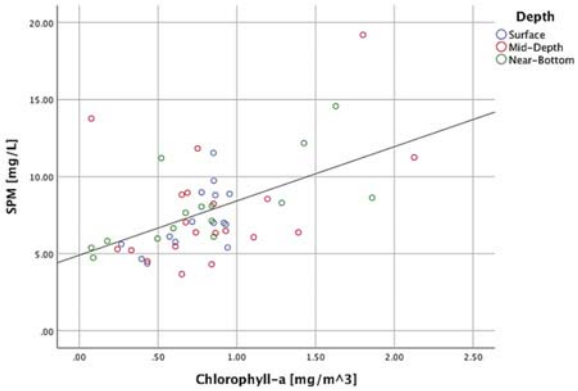

Figure 28. Suspended Particulate Matter (mg/L) plotted against chlorophyll-a, showing a linear relationship.

4.5.2. Particulate Organic Carbon and Particulate Organic Nitrogen (POC and PON):

Particulate organic carbon in the study area ranged between 4.10 and 44.52 ± 8.72 µM, with a mean value of 16.68 µM. In addition, POC showed a significant linear decrease with increasing distance from the shore (R^2 =0.40, p< 0.01) (Figure 30, a). The highest concentrations were reported near the shore, with linear decrease with distance from shore. The particulate organic carbon also showed a change with depth (R^2 =0.20, p <0.00), with a peak in increased POC at surface water (top 20 meters) (Figure 30, b).

Particulate organic nitrogen (PON) exhibited a range of 0.43 – 4.24 ± 0.85 µM, with a mean value of 1.79 µM. Furthermore, PON showed a significant linear decrease with increasing distance from the shore (R^2 =0.38, p< 0.01) (Figure 31, a). The highest concentrations was found in the shallow water and near shore while the lowest concentration was found at the deeper water and at distance from shoreline (R^2 =0.3, p<0.01) (Figure 31, b). POC and PON showed a very high significant correlation (R^2= 0.9, p <0.01).

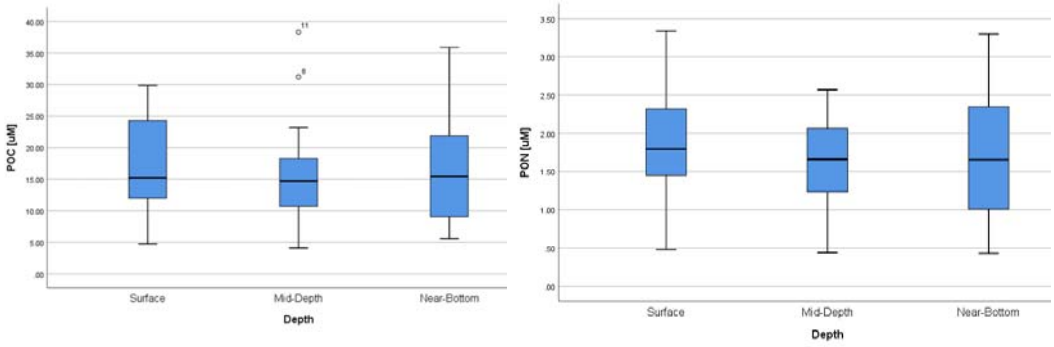

(a) (b)

Figure 29. Particulate Organic Carbon (µM) (a) and articulate Organic Nitrogen (µM) (b) distribution by depth zones (Surface, mid-depth and near-bottom water).

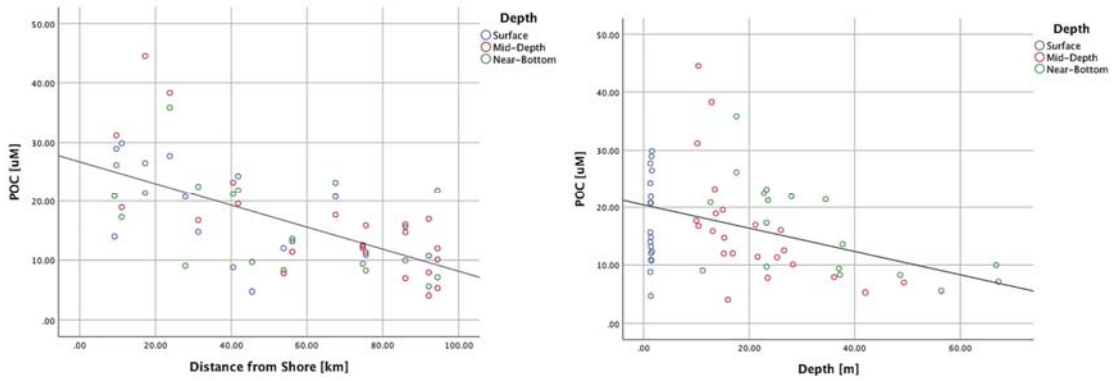

(a) (b)

Figure 30. Particulate Organic Carbon (µM) changes with distance from shore (km) (a), and with depth (m) (b).

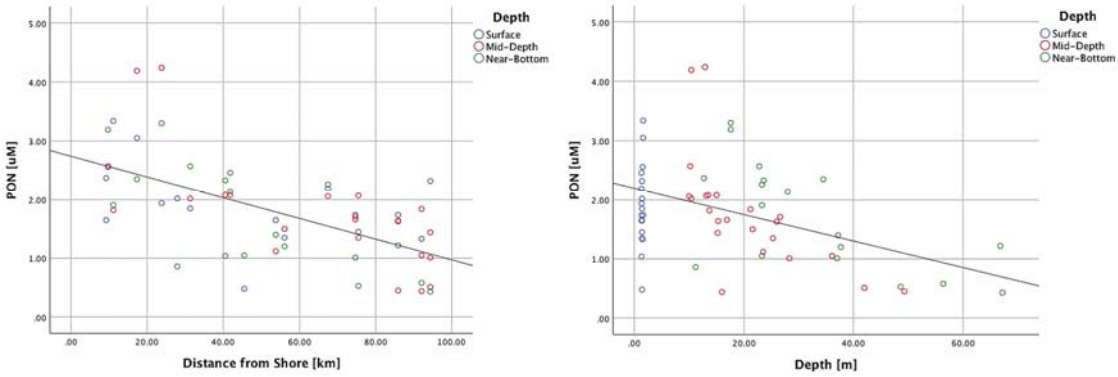

(a) (b)

Figure 31. Particulate organic nitrogen (µM) distribution along distance from the shore (km) (a), and with depth (m) (b).

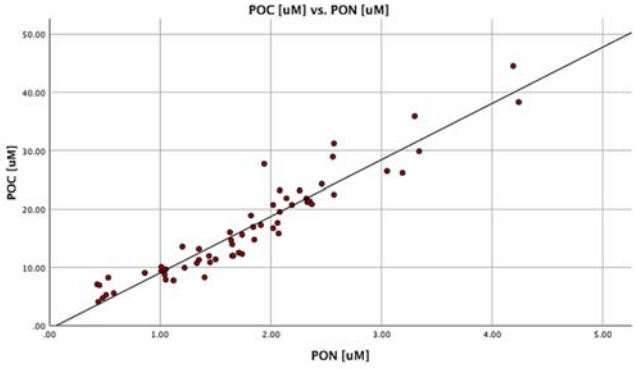

Figure 32. Correlation between particulate organic carbons (µM) and particulate organic nitrogen in the coastal zone of Qatar.

4.5.3. Carbon to Nitrogen Ratio (C:N):

Spatial and depth distribution of molar C:N ratios in the Qatari EEZ are represented in Figure 34 (a and b). The carbon to nitrogen ratio showed a wide range of 5.09 – 14.24. The average C:N molar ratio was 8.14 ± 1.76. The highest C:N ratio was reported at the deepest water of the Gulf, exceeding 13 (Figure 34, a). The highest C:N ratio was found at stations A8, B5 and C4, in the near bottom of the water column. The lowest C:N ratio was found at near bottom of B3 station.

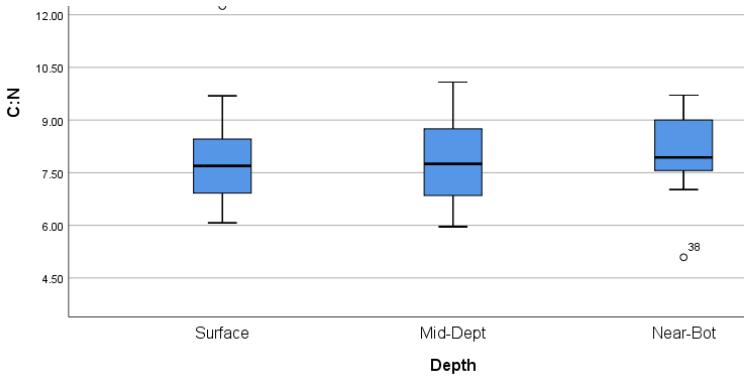

Figure 33. Changes in carbon to nitrogen ratio (C:N) in suspended particulate matter with depth zones (surface, mid-depth and near-bottom water).

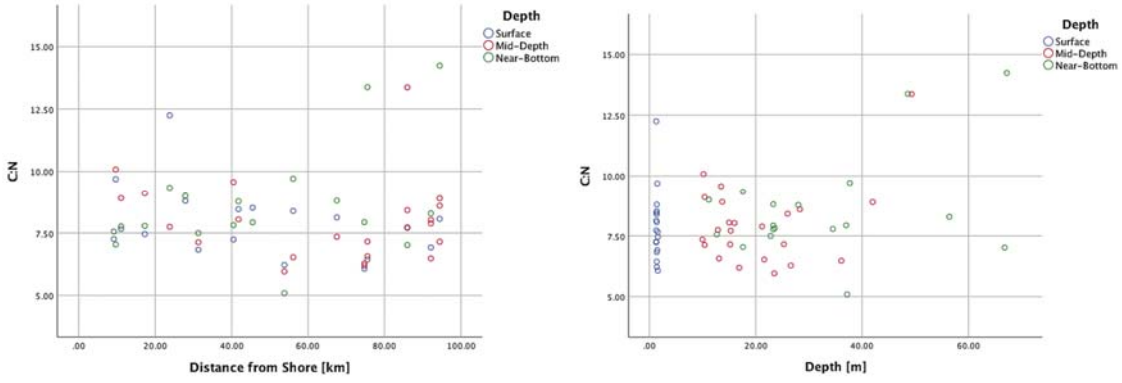

(a) (b)

Figure 34. Carbon to Nitrogen ratio (C:N) in suspended particulate matter down distance from shore (km) (a), and down depth (m) (b).

4.5.4. Carbon and Nitrogen Stable isotopes ($\delta^{13}C$ and $\delta^{15}N$):

The stable isotopes of carbon and nitrogen showed significant variability spatially and with depths ($P<0.01$) (Figures 37 and 38). Carbon stable isotope ($\delta^{13}C$) showed enrichment in the near bottom water, and depletion at the mid-depths (Figure 35). The $\delta^{13}C$ ratios ranged from -23.50 to -11.17 ‰, with a mean value of -18.56 ± 2.71 ‰. The highest $\delta^{13}C$ ratios were observed at stations B2 (near-bottom), B5 (near-bottom), and C4 (49 meters), with values of -11.17, -10.73 and -11.76 ‰, respectively. The lowest $\delta^{13}C$ ratios were found at A5 (surface), A7 (surface) and A8 (13.1 meters deep), with values of -23.26, -23.44 and -23.45 ‰, respectively.

The carbon isotope showed exponential increase with depth ($R^2= 0.21$, $p<0.01$), with a higher $\delta^{13}C$ ratios in the near bottom water (Figure 35 and 37, a). On the other hand, $\delta^{13}C$ showed no significant change with distance from shore (Figure 37, b). The carbon stable isotope $\delta^{13}C$, showed an exponential depletion with increasing temperature ($R^2 = 0.2$, $p <0.05$) (Figure 39). The nitrogen isotope had a range of -6.85 to 5.28 ± 1.77 ‰ and a mean value of 1.76 ‰, respectively. $\delta^{15}N$ showed an increase in enrichment with depth (Figure 36). Samples was most enriched with $\delta^{15}N$ near the bottom of the water column. (Figure 38, a). The samples with δ15N enrichment were found at A3, A4, A8, B5 and C4, with values of 4.60, 5.28, 4.06, 4.15, 4.15 and 4.90 ‰, respectively. Subsequently, the δ15N depletion occurred at the surface and mid-depth of A8, A9, B3 and B5, respectively. Interestingly, only station A9, showed δ15N depletion, with signatures close to zero, at the surface and the mid-depth sampling location, that's nearer to the bottom of the water column, with the values of -0.03 and -0.08 ‰. The stations that showed depletion have the values of -0.49, -0.03, -0.08, -0.34, -6.85 and -1.34 ‰, respectively. Station B4 showed the highest values of the nitrogen isotope depletion with a value of -6.85 ‰ (Figure 38, a).

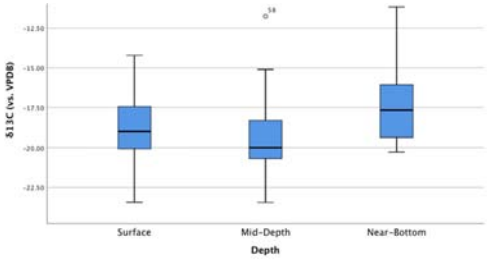

Figure 35. Changes in stable carbon isotope ($\delta^{13}C$) signature with depth zones (Surface, mid-depth and near-bottom water).

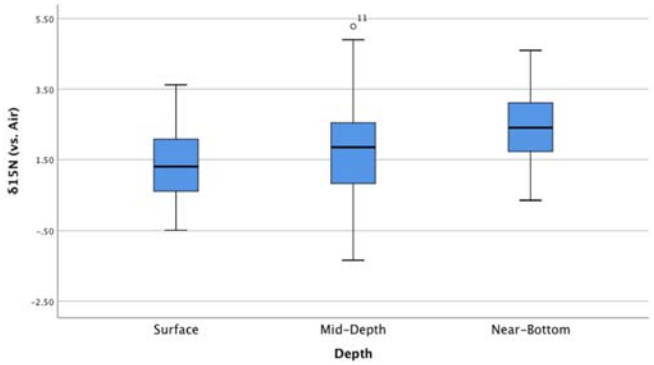

Figure 36. Changes in stable nitrogen isotope ($\delta^{15}N$) signatures with depth zones (surface, mid-depth and near-bottom water).

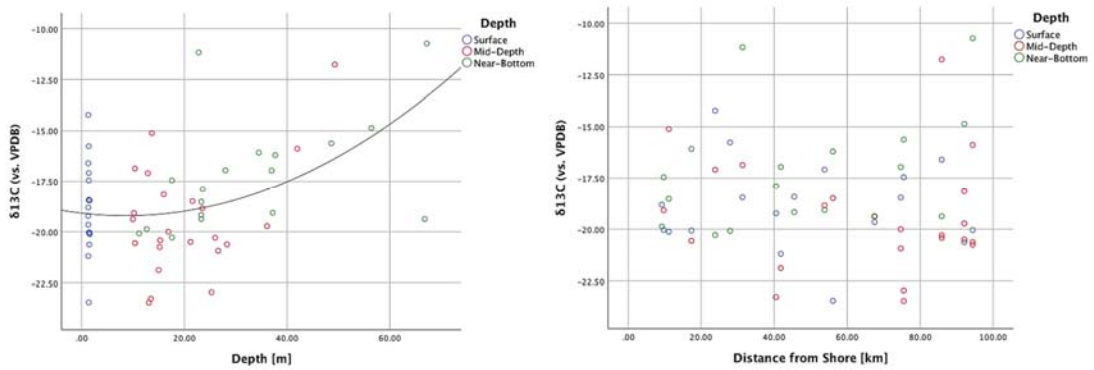

(a) (b)

Figure 37. Stable carbon isotope ($\delta^{13}C$) down depth (m) (a), and down distance from shore (km) (b).

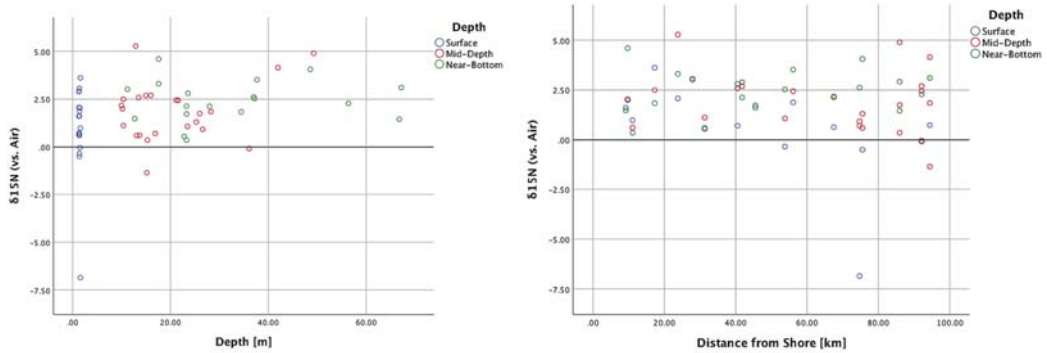

(a) (b)

Figure 38. Stable nitrogen isotope ($\delta^{15}N$) down depth (m) (a), and down distance from shore (km) (b).

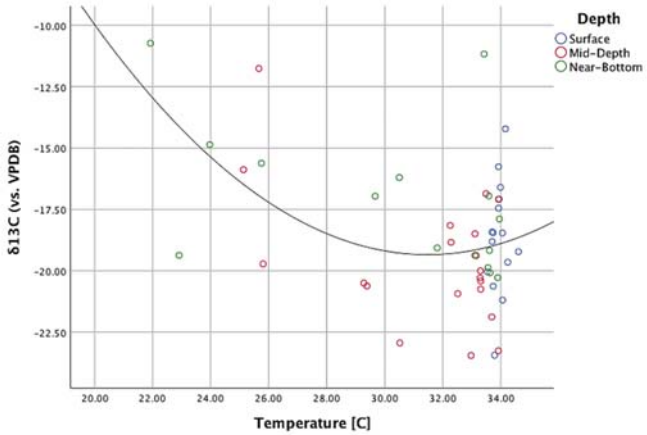

Figure 39. Changes in stable carbon isotope ratios ($\delta^{13}C$) with Temperature (°C).

CHAPTER 5: DISCUSSION:

Water T-S diagram/plots could identify three distinct water masses in the study area with apparent water stratification. The highly saline water mass of salinity >42, surface water and high temperature, slightly less saline water of salinity < 42, and bottom water of temperature less than 26 ºC and salinity less than 42 psu. Water densities of σt>28 in the present study was found only at distances beyond 80 km from the shoreline while 26<σt> 26 was common for intermediate and near bottom water in the depths between 20 meter and beyond. Formation of dense water (σt>29.5) as a dense hypersaline buoyant water in the southern Gulf around Qatar is a common feature for the Gulf Summer circulation (Kämpf, 2006). The reported density pattern showed intense stratification, which is evident in other studies that reported export of hypersaline dense water from the southern Gulf (around Qatar), toward Hormuz during late summer where it exits the Hormuz straight as bottom and intermediate water (Kämpf, 2006).

Water stratification due to warm temperature and salinity affect the water chemistry including dissolved gasses such as DO, water salinity and nutrients. Dissolved oxygen in the Gulf water showed hypoxia in the offshore bottom water. DO at any depth is a balance between air-sea exchange, productivity and respiration. Warming of the surface water decrease the oxygen solubility and it was found that 50% of DO decline in the surface oceans is related to the effect of warming (Matear and Hirst, 2003). On the other hand, warmer climate affects the respiration rate of organisms (metabolisms) which contribute to further oxygen decline. Dissolved oxygen concentration usually decreases due to either biological activity such as respiration /decomposition of OM or due to high temperature or a combination of both. The summer hypoxia in the present study was evident by the results of dissolved oxygen at the deeper waters of the EEZ in Qatar. Water is considered hypoxic when the water has dissolved oxygen concentrations less than 2.0 ml/L (Zhang et al, 2010). The levels of DO at the present study reached near 1ml/L at B central transect (B3, B4 and B5) in the near-bottom water. Water stratification diminish water mixing and intensify the decrease of the DO in the deeper water. In the present study, the low DO (<3 ml/l) was prominent only at offshore stations beyond 40 km from the shoreline, in the intermediate and deep water. The cause here is probably a combination of factors including low supply of DO to the deeper water due to stratification and low exchange due to high temperature as well as high decomposition rate of OM at the near bottom water of these locations. The extended period of summer thermocline during the

warmer season, which extends from June to September may contribute to such decrease in DO (Al-Ansari, 2015). The increase in the salinity is another factor that causes decreases in the dissolved oxygen causing zones of hypoxia that may intensify during summer. The salinity of the Gulf shows some change during the summer due to the high evaporation and limited influx of fresh water from the Tigris River and from the Gulf of Oman. Parameters such as salinity and pH showed decrease toward the north of the EEZ. The lower salinity at the north of Qatar is probably due to the fresher water influx coming from the Gulf of Oman with salinity of about 37 psu, that circulate in anti-clockwise motion. It becomes saltier and denser by the time it is near Qatar due to evaporation over time. So, as it reaches the southern coasts of Qatar, it becomes saltier compared when it was at the north. This circulation changes seasonally with the highest strength in June and the lowest in November (Ibrahim, 2017). The observed salinity, density as well as pH trends during the summer sampling for the EEZ are well explained by the circulation pattern during the summer months.

On the other hand, the observed trends of nutrients with low concentrations within 40 km from shoreline and higher concentrations at the intermediate and offshore water may be interpreted by the circulation pattern during the summer month. The anti-clock wise water current from the Gulf of Oman might be a source for the new nutrients to the oligotrophic Gulf water. Most of the measured geochemical parameters including nutrients, C:N ratios, POC, PON and stable carbon and nitrogen isotopes showed noticeable increase at the northern offshore sites of C4, B4 and A9. The high nutrients concentrations in deeper near bottom water is always related to the recycling of the nutrients at depths (Voss et al, 2013). Despite the high nutrients at the offshore stations, but most of this increase was in the deep-water, below the depth of maximum chlorophyll concentrations (Around 20-30 meters). The dissolved nutrients are essential chemical components of any aquatic environments as they necessitate the existence of life in any given aquatic environment. The lower chlorophyll in the offshore water than the near shore water (40 km from the shoreline) may be due to the light limitation below the depth of the optimum productivity of phytoplankton. The highest nitrite concentration was associated with the B3 and B4 stations, which are sites of hypoxia indicating denitrification at this hypoxic zone. Nitrite generally peaks at the bottom of sunlit zone in the ocean (Zakem et al, 2018). Denitrification peak during the summer time in many coastal regions and in lakes (Pina-Ochao and Alvarez Cobelas, 2006). The increase in nitrate concentrations with distance from shore might be due intrusion of nutrient rich water mass while the increase in nutrient with depth is

generally found due to decomposition of sinking particles at deeper water (Al-Ansari, 2015). The nutrients concentrations in the present study reflected that the Qatar EEZ has low nutrient concentrations that may be limiting the primary productivity. The dissolved nutrients concentrations in the Arabian Gulf have been investigated previously by Al-Ansari et al (2015), Hashimoto et al (1998), Brewer and Dyrssen (1985) and emphasized in a comprehensive study by Al-Yamani and Naqvi (2018). Most of the recent studies indicated that phosphate may be a limiting nutrient in the waters of the EEZ of Qatar. Dust is a major input of silicate to the marine waters of the Arabian Gulf; it is more abundant in the waters of the EEZ in Qatar. Silicate in the waters of Qatar can be influenced by inputs from the other sources including atmospheric deposits. This distance from shore and stratification are shown to limit the source of nutrients to the surface water in the offshore regions. Whereas those areas receive sources of nutrients from other means such as input from the Gulf of Oman and Shaat Al-Arab (Al-Yamani and Naqvi, 2018; Al-Ansari, 2015).

Both SPM and Chl-a concentrations where at their highest at the shallower depths within 40 km from the shore line and decreased with distance from shore. A high correlation between SPM and Chl-a indicate that Chl-a contribute significantly to the particulate organic matter production in the central Gulf. The data of stable nitrogen isotope showed that nitrogen fixation is a major source of dissolved nitrogen in the offshore region of the EEZ of Qatar. The deepest stations also show that the reduced dissolved oxygen at the bottom and mid-depths are potentially driving the remineralization of organic matter, providing nutrients at these depths, as evidenced by the high chlorophyll-a at these depths as well. Nitrate and phosphate negatively correlated with Chl-a concentrations. The lowest amounts of both nutrients were shown to have the most values of chlorophyll-a, which is attributed to the enhanced stripping of nutrients at the shallow (euphotic) region of the water column. Temperature is also evidently very important for primary production (Figure 41). The chlorophyll-a is shown to exponentially increase with temperature (R^2= 0.51, $p<0.01$), as is clearly shown in Figure 41, with most of the chlorophyll-a being found at the higher temperatures. These three factors are shown to be the most significant for primary production in the central region of the Arabian Gulf. Chlorophyll is always used as a proxy for phytoplankton biomass in the marine environment. The amount of phytoplankton can be used in a variety of ways to predict the amount of fish yield and also as indicator for the water quality. Our values of chlorophyll-a (0.08 -2.13 mg/m^3), with average amount of 0.76 ± 0.42 mg/m^3 are slightly higher than values reported by

other studies such as Abdel-Moati and Kureishy (1997) and Dorgham and Muftah (1989), (0.67 and 0.6 mg/m^3). That shows that with the amount of phytoplankton in the central Arabian Gulf didn't show significant change over the past three decades. The amount of chlorophyll-a in the central region of the Arabian Gulf is estimated to range between 0.06 – 3.83 mg/m^3 according to Hashimoto et al (1998) and MNR-Kuwait (1999), seems to be compatible with values from the present study. The maximum chlorophyll depth at the range of 20-30 meters is also evident in other local and regional studies such as Al-Naemi et al (2017). The high Chl-a concentration in the shallower depths of the study area (<25m), (0.24 to 2.13 mg/m^3) compared with the range in the deeper water (0.24 to 1.39 mg/m3) is probably related to higher nutrient availabilities at the shallower depths mainly from benthic pelagic coupling from the benthic sediments. Benthic pelagic coupling which is the exchange of nutrients and energy between the organisms of the water column and the benthic organisms. This process is more efficient in shallow water where there is a high transfer of the pelagic biomass to benthic organisms, which is coupled with a release of recycled nutrients from the sediments to the overlying water enhancing its productivity (Griffiths et al, 2018). Having the deep chlorophyll maxima, the highest amount of production in the water column around 20-30 meters depths in the study area makes the process of benthic pelagic coupling very efficient. This may explain the higher chlorophyll concentrations at shallower depths especially within 40 km of the shoreline and the low chlorophyll concentrations in stations deeper than 50 meters where recycling of nutrient to the surface water may be restricted by the water hydrodynamics and stratification. Another factor that may contribute to the high nutrients and Chl-a near the coast is proximity to coastal runoff and the proximity to the highly productive coastal wetlands such as saltmarshes, mangroves and seagrass beds. Several studies emphasized the role that coastal wetlands play in sustaining near-by ecosystems through "outwelling". Significant amount of carbon and nutrients outwell from the coastal habitats such as the mangrove to the near coastal water (Santos et al, 2019). Stratification and distance from shore restrict the amount of nutrients available to primary production in the deeper stations such as A9, B5 and C4 (Chl-a = 0.08 – 0.18 mg/$m^{3)}$. Summer thermocline contribute to limiting the productivity in the offshore region as it restricts water mixing and distribution of nutrients at the euphotic zone. Moreover, chlorophyll-a is found to be somewhat limited with little variance at the surface of the water column, with a range of 0.4 to 0.94 mg/m^3, never exceeding 1.0 mg/m^3 (Figure 37).

The mid-depth sampling sites mostly are at the chlorophyll-maximum, except in the deeper stations such as A9, B5 and C4. The mid-depth chlorophyll-a showed that the chlorophyll in

the mid-depths can reach a significant concentration of 2.13 mg/m3, which reflects highly productive areas. The peak of Chlorophyll-a at the mid-distance from the shore is probably related to factors related to nutrients delivery by the out-welling and from sediments with chlorophyll-a concentrations reaching 1.43 to 2.13 mg/m3 at the mid-depth and near-bottom depths of the water column, where these reported values occur at the chlorophyll-maximum.

The highest concentration of SPM was associated with the near bottom water in most of the stations and showed a low, yet significant correlation, with chlorophyll-a concentration ($P<0.05$). Although primary productivity partially explained the existing distribution of SPM, but apparently, SPM in the near bottom water originated from other sources beside the phytoplankton production, that is probably including microscopic heterotrophs, fecal pellets, and remains of grazing, among others. Lateral transport of sediments and SPM is also another possibility according to a measurement by Soliman et al (2019) in the central Gulf, where a near bottom lateral transport of SPM was evident. The high near the bottom SPM can be also attributed to resuspension of the marine sediments and the vertical flux of sinking particulate matter (Chester and Jickell, 2012). The SPM flux to the sediments is a main source of energy to the benthic organisms and benthic food chain. It also helps in exporting carbon from the surface water to the deep water, which is known as the biological pump, a crucial part of the carbon cycle. Furthermore, the suspended particulate matter showed a clear decrease in concentration with increasing distance from shore. As more distance is placed from the shore, productivity decreases, especially when considering that the shores are major sources of organic matter and nutrients to the marine waters. The existence of productive ecosystems such as mangroves, salt marshes, seagrasses and coral reefs in Qatar (Nasr, 2014; Sheppard et al, 1992), as well as anthropogenic inputs via sewage and wastewater, could prove to be significant source points for increased productivity.

Particulate organic carbon and nitrogen are closely related to the productivity of the marine environment. Both particulate organic carbon and nitrogen have shown to have a decrease with depth. The decrease with depth is due to the restriction of productivity towards the surface of the water column, where light, nutrients and temperature all contribute to the increased productivity. This is reflected by the surface POC and PON concentrations which have a range of 4.10 – 44.52 and 0.43 – 4.24 μM, respectively. The POC and PON have higher concentrations at the surface and mid-depths of the water column, where the nutrients and light, in addition to the hydrographical parameters provide optimum conditions for the primary

production. This is the opposite in the deeper waters, where the productivity decreases due to the loss of the optimum conditions for productivity, and the POC and PON at the bottom are a result of the sinking particles towards the sediment. Also, PON was found to be decreasing with depth with bigger variance than POC (Figures 31, b and 30, b), which can be indicative to the remineralization of nitrogen to inorganic forms by decomposers. The carbon to nitrogen ratios highest levels at the offshore locations can reflect preferential remineralization of phytoplankton. Variabilities in C:N ratios in marine environment can indicate the mixing of different sources of OM or can be due to preferential degradation of OM such as preferential degradation of nitrogen leading to high C:N ratio. The ratio of C:N is generally in the range of 6.0 – 10.0 for phytoplankton and it is less for zooplankton and bacteria. (Savoye et al, 2003). The high correlation between POC and Chl-a as well as the high C:N ratio in the present study indicate degradation of phytoplankton and an input of refractory POC from the coastal wetlands at the coasts of Qatar such as salt marshes and mangrove (Savoye et al, 2003). Since degradation of phytoplankton increases the C:N ratios making it closer to the C:N ratios of terrestrial plants, bacterial colonization on the refractory OM lowers its C:N ratios making it closer to the values of degraded phytoplankton. However, the overall average of the C:N ratio in the present study indicate that the OM in the Gulf is mainly coming from phytoplankton productivity. The C/N ratio of SPM, lack of chlorophyll-a and high levels of dissolved nutrients at those depths, indicate significant re-mineralization of organic matter, leaving refractory organic matter persisting in deeper water.

Stable carbon ($\delta^{13}C$) and nitrogen isotopes showed significant variability with space and with depth in the study area, and reflected the phytoplankton productivity in the central Gulf during the sampling period. The wide range of reported $\delta^{13}C$ (-23.45 to -11.17‰) reflects high phytoplankton productivity at the shallower sites (i.e. $\delta^{13}C$ increase) and phytoplankton degradation or export of shallow water OM from wetlands and seagrass ($\delta^{13}C$ decrease). Surface water SPM, above 50 meters, all show a $\delta^{13}C$ signatures in the range of -14.22 to -23.45 ‰, which is close to the range of the phytoplankton (O'Leary, 1981; Harmelin-Vivien, et al, 2008). However, certain samples showed slightly more enrichment in carbon isotope than the other samples, which were in the near-bottom of stations B5 and B2, and in the deepest mid-depth sampling depth (49 meters) at station C4. The enrichment in $\delta^{13}C$ can be a signal of decomposition of phytoplankton and living organisms in the deeper waters, thus giving slightly more enriched $\delta^{13}C$ signatures in SPM. Additionally, the $\delta^{13}C$ signatures obtained, prove than

most SPM is autochthonous organic matter resulting from phytoplankton productivity and possibly detritus from zooplankton grazing. The $\delta^{13}C$ of SPM was shown to be more depleted at the mid-depth of the water column (Figure 35 and 37), which is because of the phytoplankton in the chlorophyll-maximum being in large abundances at those depths. They comprise a major fraction of SPM at those mid-depths, along with the interactions of grazing and decomposition of organic matter. The $\delta^{13}C$ signatures obtained is also showing that the main source of carbon in the phytoplankton in SPM is probably due to the DIC in the seawater, which is a result of photosynthesis. This is also proven by the relatively high POC and chlorophyll-a in the waters of the EEZ, especially in certain areas towards the north-east.

The isotopic composition of suspended particulate matter shows a trend of carbon depletion and nitrogen isotope enrichment with a few exceptions for nitrogen isotopes in certain SPM in specific locations. The nitrogen isotope clearly shows that the source of nitrogen in locations A8, A9 and B3 are from nitrogen fixation. That is apparent by the signature of $\delta^{15}N$ in the suspended particulate matter which is close to zero value, the value of atmospheric nitrogen. These values of nitrogen isotope, indicate that the source of nitrogen that's incorporated into the SPM's phytoplankton and the detritus resulting from grazing on those phytoplankton, is from nitrogen fixation by nitrogen-fixing organisms such as cyanobacteria. An interesting result is the occurrence of two $\delta^{15}N$ depleted samples at the surface and deepest mid-depth samples of station A9. This depletion shows that nitrogen fixation is an important source of dissolved nitrogen at the north-eastern part of the Qatari EEZ. The other stations that had depletion in $\delta^{15}N$ were stations B4 and B5. The depletion was much higher than the other stations, with a surface and mid-depth $\delta^{15}N$ signatures of -6.85 and -1.34 for B4 and B5. This $\delta^{15}N$ depletion can mean that the source of the nitrogen in these areas are from remineralization of PON and SPM at the shallow region of the water, which is also corroborated by the decrease in PON at the sites of these stations and the increase of dissolved nitrogen that's available at the lower depths. The high $\delta^{15}N$ (0.36 – 5.28) at the rest of the sites may indicate enriched sources of nitrogen. The signatures of $\delta^{15}N$ are within the known range of phytoplankton, and indicating their significant contribution to the formation of SPM in the central Arabian Gulf.

CHAPTER 6: CONCLUSION:

Sources and distributions of suspended particulate matter (SPM) during the summer of 2019, were investigated using integrated measurements of biogeochemical parameters of seawater in the Exclusive Economic Zone of Qatar. Concentrations of SPM, POC, PON, Chl-a, dissolved nutrients (ammonia, nitrite, nitrate, phosphate, silicate) were measured in 18 locations in three transect off the east coast of Qatar. Levels, depth patterns and distance from shore trends were all linked to the physiochemical parameters including DO, salinity, temperature and density. Levels of SPM showed significant changes with depth and with distance from shore. Stable isotopes of carbon and nitrogen in SPM were used to trace the sources of SPM in the study area. Ratios of carbon and nitrogen isotopes showed the importance of the primary productivity at near shore areas toward the POC and PON production, and in the export of matter from the shore to the marine waters in the Exclusive Economic Zone in Qatar via lateral transport. Values of Chlorophyll-a concentration indicated that the central Arabian Gulf is relatively productive as a result of the existence of favorable condition allowing for enhanced productivity during the summer season. The C/N ratio showed the mixed origin of the SPM in the Gulf. Stable isotopes of $\delta^{13}C$ and $\delta^{15}N$ showed that the majority of the organic matter in the central Arabian Gulf are originated from primary productivity. Signatures of $\delta^{15}N$ showed that nitrogen fixation plays a significant role in introducing new nitrogen to the oligotrophic Gulf basin. Concentrations of the nutrients in the Gulf were also influenced by proximity to the coast, showing increase with increasing depth and distance. This indicate inputs from sources such as remineralization and nitrogen fixation, as well as inputs from the Gulf of Oman. Silicate is not limited in the Gulf with significant input from the dust in the atmosphere. Water temperature and density during summer play a significant role in limiting migration of SPM, POC, PON and chlorophyll-a to the deeper parts of the water column, and preventing dissolved nutrients from cycling up to the upper layers of the water column.

REFERENCES:

1. Abdel-Moati, M.A. R., Kureishy, T. W. (1997). Dissolved copper, cadmium and lead in the coastal waters of Qatar, Arabian Gulf. Indian Journal of Marine Sciences. Vol. 26. pp 143-149.
2. Al-Ansari, E. M. A. S., Rowe, G., Abdel-Moati, M. A. R., Yigiterhan, O., Al-Maslamani, I., Al-Yafei, M. A., AL-Shaikh, I., Upstill-Goddard, R. (2015). Hypoxia in the central Arabian Gulf Exclusive Economic Zone (EEZ) of Qatar during summer season. Estuarine, Coastal and Shelf Science. Vol. 159. pp 60-68.
3. Al-Maslamani, I., Le Vay, L. (2007) Feeding Ecology of the grooved tiger shrimp Penaeus semisulcatus De Haan (Decapoda: Penaeidae) in inshore waters of Qatar, Arabian Gulf. Marine Biology. Vol. 150. Issue 4. pp 627-637.
4. Al-Naimi, N., Raitsos, D. E., Ben-Hamadou, R., Soliman, Y. (2017, March 22). Evaluation of Satellite Retrievals of Chlorophyll-*a* in the Arabian Gulf. Remote Sensing. Vol. 9. Issue 301.
5. Al-Yamani, F., Naqvi, S. W. A. (2018, In Press). Chemical Oceanography of the Arabian Gulf. Deep Sea Research Part II: Topical Studies in Oceanography. Retrieved from https://www.sciencedirect.com/science/article/pii/S096706451730400 9#!
6. Boyd, P. W. (2015, October 13). Toward quantifying the response of the ocean's biological pump to climate change. Frontiers in Marine Sciences. Vol. 2.
7. Brewer, P. G., Dyrssen, D. (1985). Chemical oceanography of the Persian Gulf. Progress in Oceanography. Vol. 14. pp 41-55.
8. Chafetz, H. S., McIntosh, A. G., Rush, P. F. (1988). Freshwater phreatic diagenesis in the marine realm of Recent Arabian Gulf carbonates. Journal of Sedimentary Research. Vol. 58. Issue 3. pp 433-440. Retrieved from https://pubs.geoscienceworld.org/sepm/jsedres/article-abstract/58/3/433/98031
9. Chafetz, H. S., Rush, P. F. (1994) Diagenetically altered sabkha-type Pleistocene dolomite from the Arabian Gulf. Sedimentology. Vol. 41. Issue 3. Retrieved from https://onlinelibrary.wiley.com/doi/abs/10.1111/j.1365-3091.1994.tb02003.x

10. Carpenter, J. H. (1965). Technique for the Winkler oxygen method. Limnology and Oceanography. Vol. 10. pp 141-143.
11. Carpenter, J. H. (1965). The Accuracy of the Winkler Method for Dissolved Oxygen Analysis. Limnology and Oceanography. Vol. 10. Issue 1. pp 135-140.
12. Chester, R., Jickells, T. (2012) Marine Geochemistry. Third Edition. Wiley-Blackwell. USA. pp 185-186
13. Dorgham, M. M., Muftah, A. (1989). Environmental conditions and phytoplankton distribution in the Arabian Gulf and Gulf of Oman, September 1986. Journal of the Marine Biological Association of India. Vol. 31. Issues 1&2. pp 36-53.
14. Emerson, S. R., Hedges, J. I. (2008). Chemical Oceanography and the Marine Carbon Cycle. Cambridge University Press. UK.
15. Erftemeijer, P., Shuail, D. A. (2012). Seagrass habitats in the Arabian Gulf: distribution, tolerance thresholds and threats. Aquatic Ecosystems Health and Management. Vol. 15. pp 73-83.
16. Gökçe, D. (2016, June 29). Algae as an Indicator of Water Quality. Algae – Organisms for Imminent Biotechnology. IntechOpen.
17. Grashoff, K., Kremling, K., Ehrhardt, M. (1999). Methods of Seawater Analysis. Third, Completely Revised and Extended Edition. WILEY-VCH. Germany.
18. Griffiths, J. R., Kadin, M., Nascimento, F. J. A., Tamelander, T., Törnoos, A., Bonaglia, S., Bonsdorff, E., Brüchert, V., Gärdmark, A., Järnström, M., Kotta, J., Lindgren, M., Nordström, M. C., Norkko, A., Olsson, J., Weigel, B., Žydelis, R., Blenckner, T., Niiranen, S., Winder, M. (2017). The importance of benthic-pelagic coupling for marine ecosystem functioning in a changing world. Global Change Biology. Vol. 23. Issue 6. pp 2179-2196.
19. Gupta, A. S., McNeil, B. (2012). Chapter 6 - Variability and Change in the Ocean. The Future of the World's Climate. Second Edition. pp 141-165.
20. Hama, T., Miyazaki, T., Ogawa, Y., Iwakuma, Y., Takahashi, M., Otsuki, A., Ichimura, S. (1983). Measurement of Photosynthetic Production of a Marine Phytoplankton Population Using as Stable ^{13}C Isotope. Marine Biology. Vol. 73. pp 31-36. Retrieved from https://link.springer.com/article/10.1007/BF00396282
21. Harmelin-Vivien, M., Loizeau, V., Mellon, C., Beker, B., Arlhac, D., Bodiguel, X., Ferraton, F., Hermand, R., Philippon, X., Salen-Picard, C. (2008). Comparison of C and N stable isotope ratios between surface particulate organic matter and

microphytoplankton in the Gulf of Lions (NW Mediterranean). Continental Shelf Research. Vol. 28. pp 1911-1919.

22. Holail, H. (1999) The isotopic composition and diagenetic history of pleistocene carbonates, North Qatar. Carbonates and Evaporates. Vol. 14. Issue 41. Retrieved from https://link.springer.com/article/10.1007/BF03176147
23. Holail, H., Shaaban, M. N., Mansour, A. S., Rifai, R. I. (2005). Diagenesis of the Middle Eocene Upper Dammam Subformation, Qatar: Petrographic and isotopic evidence. Carbonates and Evaporates. Vol. 20. Issue 1. pp 72-81. Retrieved from https://link.springer.com/article/10.1007/BF03175450
24. Huang, C., Jiang, Q., Yao, L., Yang, H., Lin, C., Huang, T., Zhu, A. X., Zhang, Y. (2018). Variation pattern of particulate organic carbon and nitrogen in oceans and inland waters. Biogeosciences. Vol. 15. pp 1827-1841.
25. Hughes, E. H., Sherr, E. B. (1983). Subtidal food webs in a Georgia estuary: $\delta^{13}C$ analysis. Journal of Experimental Marine Biology and Ecology. Vol. 67. pp 227-242.
26. Ibrahim, H. D. (2017). Investigate of the impact of desalination on the salinity of the Persian Gulf. Massachusetts Institute of Technology. Department of Civil and Environmental Engineering. USA.
27. Jeffrey, S. W., Humphrey, G. F. (1975). New spectrophotometric equations for determining chlorophylls a, b, c_1, c_2 in higher plants, algae and natural phytoplankton. Biochemie und Physiologie der Pflanzen. Vol. 167. Issue 2. pp 191-194.
28. Jenkins, W. J. (2001). Tracers of Ocean Productivity. Encyclopedia of Ocean Sciences. Second Edition. Academic Press. pp 93-99. Retrieved from https://www.sciencedirect.com/science/article/pii/B9780123744739001740
29. Kämpf, J., Sadrinasab, M. (2006). The circulation of the Persian Gulf: a numerical study. Ocean Science. Vol. 2. pp 27-41.
30. Khalaf, F., Literathy, P., Al-Bakri, D., Al-Ghadban, A. (1986). Total organic carbon distribution in the Kuwait marine bottom sediments. Marine Environment and Pollution. Proceedings of the First Arabian Gulf Conference on Environemnt and Pollution. Kuwait University. Faculty of Sciences. KFAS and EPC. Kuwait. pp 117-126.
31. Kürten, B., Al-Aidaroos, A. M., Struck, U., Khomayis, H. S., Gharbawi, W. Y., Sommer, U. (2014). Influence of environmental gradients on C and N stable isotope ratios in coral reed biota of the Red Sea, Saudi Arabia. Journal of Sea Research. Vol.

85. pp 379-394.

32. Le Vay, L., Gamboa-Delgado, J. (2011). Naturally-occurring stable isotopes as direct measures of larval feeding efficiency, nutrient incorporation and turnover. Aquaculture. Vol. 315. Issue 1. pp 95-103.

33. Levin, L. A., Currin, C. (2012). Stable Isotope Protocols: Sampling and Sample Processing. UC San Diego. Scripps Institution of Oceanography.
34. Levinton, J. (2011). Marine Biology: Function, Biodiversity, Ecology. International Third Edition. Oxford University Press.
35. Libes, S. M. (2009). Introduction to Marine Biogeochemistry. Second Edition. Academic Press. Elsevier. USA. pp 208-2011
36. Libes, S. M. (1983). Stable isotope geochemistry of nitrogen in marine particulates. Woods Hole Oceanographic Institution. Massachusetts Institute of Technology. USA.
37. Limits in the Seas. (1981, September 11). Continental Shelf Boundaries: The Persian Gulf. United States Department of State. Bureau of Intelligence and Research. USA.
38. Liu, Q., Kandasamy. S., Lin, B., Wang, H., Chen, C. A. (2018). Biogeochemical characteristics of suspended particulate matter in deep chlorophyll maximum layers in the southern East China Sea. Biogeosciences. Vol. 15. pp 2091-2109.
39. Matear, R., Hirst, A. C. (2003)> Long-term changes in dissolved oxygen concentrations in the ocean caused by protracted global warming. Global Biogeochemical Cycles. Vol. 17. Issue 4.
40. MNR-Kuwait. (1999). Marine National Report-National Report on the State of the Marine Environment in Kuwait. Environmental Public Authority. Kuwait.
41. Murphy, J., Riley, J. P. (1962). A modified single solution for the determination of phosphate in natural waters. Analytica Chimica Acta. Vol. 27. pp 31-36.
42. Nasr, H. A. (2014, May 14). Marine Ecosystem Diversity in the Arabian Gulf: Threats and Conservation. IntechOpen.
43. Nutrient Analysis in Tropical Marine Waters: Practical guidance and safety notes for the performace of dissolved micronutrient analysis in sea water with particular reference to tropical waters. (1993). Intergovermental Oceanographic Commision (IOC). UNESCO.
44. Nybakken, J. W. (2001). Marine Biology: An Ecological Approach. Fifth Edition. Benjamin Cummings.

45. O'Leary, M. H. (1981). Carbon isotope fractionation in plants. Phytochemistry. Vol. 20. pp 553-567.
46. Oceans and the Carbon Cycle. EarthLabs
47. Oceans and the Carbon Cycle. EarthLabs. Retrieved from https://serc.carleton.edu/eslabs/carbon/6a.html
48. Ogric, N., Fontolan, G., Faganeli, J., Covelli, S. (2005). Carbon and nitrogen isotope compositions of organic matter in coastal marine sediments (the Gulf of Trieste, N Adriatic Sea): indicators of sources and preservation. Marine Chemistry. Vol. 95. pp 163-181.
49. Parsons, T. R., Maita, Y., Lalli, C. M. (1984). A Manual of Chemical and Biological Methdods for Sea Water Analysis. Pergamon Press. pp 3-25.
50. Piña-Ochoa, E., Álvarez-Cobelas, M. (2006, July 12). Denitrification in Aquatic Environments: A Cross-system Analysis. Biogeochemistry. Vol. 81. pp 111-130.
51. Price, A. R. G., Sheppard, C. R. C., Roberts, C. M. (1993). The Gulf: Its biological setting. Marine Pollution Bulletin. Vol. 27. pp 9-15.
52. Riegl, B. M., Purkis, S. J. (2012). Coral Reefs of the Gulf: Adaptation to Climatic Extremes. Coral Reefs of the Gulf. Vol. 3. pp 349-374.
53. Santos, I. R., Maher, D. T., Larkin, R., Webb, J. R., Sanders, C. J. (2019, January 2). Carbon outwelling and outgassing vs. burial in an estuarine tidal creek surrounded by mangroves and saltmarsh wetlands. Limnology and Oceanography. Vol. 64. Issue 3.
54. Savoye, N., Aminot, A., Tréguer, P., Fontugne, M., Naulet, N., Kéroul, R. (2003). Dynamics of particulate organic matter δ^{15} N and δ^{13} C during spring phytoplankton blooms in a macrotidal ecosystem (Bay of Seine, France). Marine Ecology Progress Series. Vol. 255. pp 27-41.
55. Schubert, C. J., Calvert, S. E. (2001). Nitrogen and carbon isotopic composition of marine and terrestrial organic matter in Arctic Ocean sediments: implications for nutrient utilization and organic matter composition. Deep Sea Research I. Vol. 48. pp 789-810.
56. Sheppard, C., Price, A., Roberts, C. (1992). Marine Ecology of the Arabian Region: Patters and processes in extreme tropical environments. Academic Press. United Kingdom. pp 141-160.
57. Sigman, D. M., Hain, M. P. (2012). The Biological Productivity of the Ocean. Nature Education. Vol. 3, Issue 6. pp 1-16.

58. Soliman, Y. S., Alansari, E. M. A., Sericano, J. L., Wade, T. L. (2019, March 25). Spatio-temporal distribution and sources identifications of polycyclic aromatic hydrocarbons and their alkyl homolog in surface sediments in the central Arabian Gulf. Science of The Total Environment. Vol. 658. pp 787-797.
59. Sollai, M., Hopmans, E. C., Schouten, S., Keil, R. G., Damsté, J. S. S. (2015). Intact polar luipids of Thaumarchaeota and ananmmox bacteria as indicators of N cycling in the eastern tropical North Pacific oxygen-deficit zone. Biogeosciences. Vol. 12. pp 4725-4737.
60. Solorzano, L. (1969). Determination of Ammonia in Natural Waters by the Phenolhypochlorite Method. Limnology and Oceanography. Vol. 14. pp 799-801,
61. Strickland J. D. H., Parsons, T. R. (1972). A Practical Handbook of Seawater Analysis. Second Edition. Fisheries Research Board of Canada Ottawa 1972. Bulletin 167.
62. Valiela, I. (1995). Factors Affecting Primary Production. Marine Ecological Processes. Springer. USA. pp 36-83.
63. Vaughan, G. O., Al-Mansoori, N., Burt, J. A. (2019). Chapter 1 – The Arabian Gulf. World Seas: an Environmental Evaluation (Second Edition). Volume II: the Indian Ocean to the Pacific. pp 1-23.
64. Villegas, I., de Giner, G. (1973). Phytoplankton as a biological indicator of water quality. Water Research. Vol. 7. Issue 3. pp 479-487.
65. Voss, M, Bange, H. W., Dippner, J. W., Middelburg, J. J., Montoya, J. P., Ward, B. (2013, July 5). The marine nitrogen cycle: recent discoveries, uncertainties and the potential relevance of climate change. Philosophical Transactions of the Royal Society B. Royal Society Publishing.
66. Walton, M. E. M., Al-Maslamani, I., Haddaway, N., Kennedy, H., Castillo, A., Al-Ansari, E. S., Al-Shaikh, I., Abdel-Moati, M., Al_Yafei, M. A. A., Le Vay, L. (2017). Extreme ^{15}N Depletion in Seagrasses. Estuaries and Coasts. Vol. 39. Issue 6. pp 1709-1723. Retrieved from https://link.springer.com/article/10.1007/s12237-016-0103-3
67. Winkler, L. W. (1888). Die Bestimmung des in Wasser gelösten Sauerstoffen. Berichte der Deutschen CHemischen Gesellschaft. Vol 21. pp 2843 -2855.
68. Yurtsever, Y., Payne, B. R. (1979). Application of environmental isotopes togroundwater investigations in Qatar. International Atomic Energy Agency (IAEA). IAEA.
69. Zakem, E. J., Al-Haj, A., Church, M. J., van Dijken, G. L., Dutkiewicz, S., Foster, S.

Q., Fulweiler, R. W., Mills, M. M., Follows, M. J. (2018, March 23). Ecological control of nitrite in the upper ocean. Nature Communications. Vol. 9. Issue. 1206.

70. Zhang, J., Gilbert, D., Gooday, A. J., Levin, L., Naqvi, S. W. A., Middelburg, J. J., Scranton, M., Ekau, W., Pena, A., Dewitte, B. (2010). Natural and human-induced hypoxia and consequences for coastal areas: synthesis and future development. Biogeosciences. Vol. 7. pp 1443-1467.